



Original Article

Synergistic neuroprotective effects of two natural medicinal plants against CORT-induced nerve cell injury by correcting neurotransmitter deficits and inflammation imbalance

Jin Pan^{a, #}, Yanting Lu^{a, #}, Sijia Wang^{b, #}, Ting Ma^c, Xiaoyan Xue^a, Zhe Zhang^a, Qiancheng Mao^a, Dongjing Guo^a, Ke Ma^{a, *}

^a College of Chinese Medicine, Shandong University of Traditional Chinese Medicine, Jinan 250355, PR China

^b College of Acupuncture and Tuina, Shandong University of Traditional Chinese Medicine, Jinan 250355, PR China

^c College of Rehabilitation, Shandong University of Traditional Chinese Medicine, Jinan 250355, PR China



ARTICLE INFO

Keywords:

Nerve cell injury model
Neuroprotection
Lilium henryi Baker (Liliaceae)
Rehmannia glutinosa (Gaertn.) DC. (Plantaginaceae)
Bioactive compounds
Gama-aminobutyric acid

ABSTRACT

Background: *Lilium henryi* Baker (Liliaceae) and *Rehmannia glutinosa* (Gaertn.) DC. (Plantaginaceae) were the traditional natural medicinal plants for the treatment of depression, but the antidepressant mechanism of two plants co-decoction (Also known as Lily bulb and Rehmannia decoction (LBRD) drug-containing serum (LBRDDS) has not been elucidated in the *in vitro* model of depression.

Material and methods: Here, UHPLC-Q-TOF/MS was used to identify the active components of LBRDDS and the potential effector substance was identified by bioinformatics analysis. CORT-induced nerve cells cytotoxicity was used to investigate the neuroprotection effect of LBRDDS and the underlying pharmacological mechanisms were explored by multiple experimental methods such as molecular docking, immunofluorescence, gain- or loss-of function experiments.

Results: Bioactive compounds in LBRDDS absorbed from intestinal tract were transformed or metabolized by the gut microbiota including palmitic acid, adrenic acid, linoleic acid, arachidonic acid and docosapentaenoic acid. Network pharmacology analysis and molecular docking showed fatty acid metabolism, neurotransmitter synthesis and neuroinflammation may be potential therapeutic targets of LBRDDS. LBRDDS can improve the activity of model cells, reduce cytotoxicity of lactate dehydrogenase, recover neurotransmitter imbalance, relieve inflammatory damage, down-regulate the expression of miRNA-144-3p, increase the mRNAs and protein expression level of Gad-67 and VGAT, and promote the synthesis and transport of GABA.

Conclusion: Therefore, LBRDDS exerts neuroprotective effects by correcting neurotransmitter deficits and inflammation imbalance in the CORT-induced nerve cell injury model.

Introduction

Depression is a serious mood disorder, characterized by persistent feeling of sadness and loss of interest. It usually results in a variety of psycho-somatic symptoms, with high recurrence rate, high suicide rate, and high mortality, and therefore it brings a heavy economic burden to the society (Goodwin et al., 2022; Jha and Mathew, 2023; Mokhtari,

2022). It affects a wide range of people. The etiology of depression is complex, and involves interactions between multiple systems. Modern studies have shown that the pathogenesis of depression mainly involves neuroimmune inflammation, hormone secretion disorders, hypothalamic-pituitary-adrenal (HPA) axis dysfunction, excitatory and inhibitory (E/I) neural circuit abnormalities, monoamine neurotransmitter imbalance, gut microbiota imbalance, etc. (Li et al., 2022; Lin

Abbreviation: LDH, Lactate dehydrogenase; LBRD, Lily Bulb and Rehmannia Decoction; LBRDDS, Lily Bulb and Rehmannia Decoction medicated serum; 5-HT, 5-hydroxytryptamine; GABA, Gama-aminobutyric acid; Glu, Glutamic acid; IL-1 β , Interleukin 1 β ; IL-10, Interleukin 10; KEGG, Kyoto encyclopedia of genes and genomes; E/I, Excitatory and inhibitory; VGAT, Vesicular GABA transporter; Gad67, Glutamate decarboxylase 67; HPA, Hypothalamic-pituitary-adrenal; TCM, Traditional Chinese medicine.

* Corresponding author.

E-mail address: make@sdutcm.edu.cn (K. Ma).

These authors contributed equally to this work.

<https://doi.org/10.1016/j.phymed.2023.155102>

Received 2 June 2023; Received in revised form 30 August 2023; Accepted 17 September 2023

Available online 18 September 2023

0944-7113/© 2023 Elsevier GmbH. All rights reserved.

et al., 2022; Liu et al., 2023; Lu et al., 2023; Medina-Rodriguez et al., 2023). Currently, antidepressant drugs are usually expensive, limited in selection and slow in effect with side effects such as drowsiness, gastrointestinal reactions, cardiovascular diseases, sexual dysfunction, etc. (Gonda et al., 2023; Zhang et al., 2022a).

Chinese medicinals have played a significant role in the clinical treatment of depression with the characteristics of multi-component, multi-target, strong synergistic effect and few side effects. In recent years, Chinese medicinals have been widely used worldwide for its unique multi-target efficacy. It is expected to supplement or substitute antidepressant drugs, and therefore it has attracted wide attention from researchers (Wang et al., 2019; Xia et al., 2021). LBRD, first recorded in *Synopsis of Golden Chamber* by Zhang Zhongjing, is composed of *Lilium henryi* Baker (Liliaceae) bulb and raw juice from *Rehmannia glutinosa* (Gaertn.) DC. (Plantaginaceae), with the effect of nourishing yin and moisturizing lung, purging heart and soothing mind. In our previous study, the main active components of LBRD were detected by UHPLC-Q-TOF/MS, including vidarabine, amino adipic acid, myristic acid, catalpol, verbascoside, coumarin, etc. Among them, the contents of verbascoside and catalpol met the standard qualities of *L. henryi* Baker and *R. glutinosa* required by the Pharmacopoeia of People's Republic of China (2020 Edition). Thus, verbascoside and catalpol may be served as quality control marker and effective ingredients of LBRD.

According to modern research and clinical studies, LBRD is of good antidepressant effects. It could enhance hippocampal synaptic plasticity in a rat depression model established by using corticosterone (CORT) and chronic constraint stress (Zhao et al., 2021). In addition, it could regulate the synthesis and release of gamma-aminobutyric acid (GABA) mediated by miRNA-144-3p to attenuate somatostatin interneurons deficits so as to play an antidepressant role (Xue et al., 2022). The antidepressant mechanisms of LBRD usually involve increasing the content of monoamine neurotransmitters, alleviating oxidative stress response, regulating circadian rhythm, enhancing neurotrophic signaling pathway, antagonizing overactivation of HPA axis, and inhibiting inflammatory response (Chen et al., 2012; Miao et al., 2019; Zhang et al., 2020; Zhang et al., 2021a).

The pharmacodynamics research of drug-containing serum is controversial since the material basis is not clear, and it is difficult to study the distribution, metabolism and transformation of components in Chinese medicinals after absorption into the blood, as well as to study how such components cross brain-blood barrier. Moreover, there are few cell models of depression, mainly through simulating the pathogenesis of depression using chemical drugs such as hydrogen peroxide or hormone drugs to cause certain damages to nerve cells, such as increased inflammation level, neurotransmitter disorder or insufficiency, elevated oxidative stress level (Correia et al., 2022; Shi et al., 2019; Yang et al., 2022a). Therefore, we first identified the active components of Lily Bulb and *Rehmannia* Decoction drug-containing serum (LBRDDS) and then analyzed the changes of gut microbiota after oral administration of LBRD. Combining network pharmacology with molecular docking technology, we constructed an evidence chain of composition, molecular target, gut microbiota, metabolic pathway and neurotransmitter to comprehensively explore the pharmacological mechanism of the antidepressant effect of LBRDDS. Since CORT can cause neurotransmitter loss and inflammatory activation to induce depression, nerve cells damaged by CORT are used to construct a cell model suitable for studying the *in vitro* antidepressant pharmacological mechanism of Chinese medicinals drug-containing serum, which can simulate the E/I imbalance of depression and the pathological mechanism of inflammatory injury. Subsequently, the protective effect of LBRDDS on the cell model was verified by detecting the levels of neurotransmitters and inflammatory factors as well as expression levels of key genes and proteins.

Materials and methods

Chemicals and reagents

CCK8 (Med ChemExpress, Jersey, USA); CORT (Med ChemExpress, Jersey, USA); DMEM-F12, neurobasal, GlutaMAX™, fetal bovine serum, trypsin enzyme (Gibco, Carlsbad, US); PBS buffer (Servicebio Biotechnology Co., LTD., Wuhan, China); LDH enzyme activity assay kit, enzyme-linked immunosorbent assay kit (Jingmei Biotechnology Co., LTD., Jiangsu, China); lipofectamine™ 3000 (Invitrogen, Carlsbad, US); super signal HRP (Thermo Fisher, Waltham, US); cell-specific RNA extraction kit (SparkJade Biotechnology Co., Ltd, Shandong, China); BeyoFast™ SYBR Green One-Step qRT-PCR kit (Beyotime Biotechnology, Shanghai, China); miRNA fluorescence quantitative PCR kit (Sango Biotech, Shanghai, China).

Preparation of LBRD drug-containing serum

LBRD was prepared according to the method described previously (Chi et al., 2019; Zhang et al., 2020). LBRD decoction is composed of fresh *L. henryi* Baker (Liliaceae) bulb from Shennongjia (Shennongjia Organic Specialty Shop, Hubei Province, China), and raw *R. glutinosa* (Plantaginaceae) root from Jiaozuo (Jiaozuo Huaiyao Co., Ltd. Henan Province, China). Two Chinese medicinals were verified by Shandong Provincial Analysis and Testing Center using molecular biology techniques and traditional methods. For the identification and quality report of medicinal materials, please refer to official number SFW201892 in the Supplementary Figure 1. The preparation procedures were described in our previous study (Zhang et al., 2020). Four hundred grams of fresh *L. henryi* Baker bulb was soaked in water overnight, and then decocted to obtain 200 ml decoction, and 400 g fresh *R. glutinosa* root was extracted to obtain 200 ml raw *R. glutinosa* juice. Finally, *L. henryi* Baker bulb decoction and raw *R. glutinosa* juice were mixed and decocted to obtain 300 ml decoction. The specific preparation process is detailed in Supplementary Figure 2. The specimens of *L. henryi* Baker bulb (No. SDUTCM, 20220109-01) and raw *R. glutinosa* root (No. SDUTCM, 20220115-04) were stored at Shandong Co-Innovation Center of Classic TCM Formula, Shandong University of Traditional Chinese Medicine.

Experiments were performed on male SD rats weighing (200–220 g) obtained from Beijing Vital River Laboratory Animal Technology Co., Ltd. (Beijing, China). The rats were reared adaptively for one week, and the state of controlled environmental conditions were as follows: constant temperature 22±2°C, relative humidity 55±5 %, free eating and drinking, 12 h light/dark cycle. Then 20 rats were randomly divided into blank serum group and LBRDDS group. The administration dose of LBRD was calculated according to the body surface area. The daily dose for gavage was 90 g/kg, and the blank group was given the same amount of normal saline for gavage and rats were gavaged twice a day for four days. One hour after the last administration, rats were anesthetized with isoflurane. Blood samples were collected from the abdominal aorta and were allowed to stand at room temperature for 1 h. After that, blood samples were centrifuged at 3500 rpm for 10 min at 4°C to isolate serum. The obtained serum was inactivated at 56°C for 30 min, then filtrated a 0.22 µm filter, and stored at -20°C for later use.

LBRDDS composition analysis

Fifty microliters of LBRDDS were added with 200 µl of methanol, then vortexed for 10 min, and centrifuged for 10 min at 4°C. The supernatant was further analyzed. The mass spectrometry conditions were as follows: ion source: electrospray ionization source (ESI) scanning method: positive and negative ion switching scanning detection method: full mass/dd-MS2, resolution: 70000 (full mass); 17500 (dd-MS2); scan range: 100.0~1500.0 m/z; spray voltage: 3.2 kv (positive, negative); capillary temperature: 300°C; collision gas: high-purity argon (purity ≥ 99.999 %); normalized collision energy (NCE): 30 %; sheath gas:

nitrogen (purity $\geq 99.999\%$), 40 arb; auxiliary gas: nitrogen (purity $\geq 99.999\%$), 15 arb; 350°C. The mass chromatographic conditions were as follows: conditions: column: AQ-C18, 150 \times 2.1 mm, 1.8 μm ; flow rate: 0.30 ml/min; aqueous phase: 0.1 % formic acid; organic phase: methanol; column; oven temperature: 35°C; autosampler temperature: 10.0°C; autosampler injection volume: 5 μl .

Gut microbiota analysis

After the drug-containing serum extraction was completed in rats in the blank group and LBRDDS group, the cecal contents were collected for 16S rRNA sequencing, with three samples per group. This sequencing services were provided by Shanghai Paisenol Biotechnology Co., Ltd. After DNA from the samples was extracted, the quantity of the DNA samples was measured using a NanoDrop spectrophotometer (Thermo, A30221), and the quality of the DNA samples was measured using agarose gel electrophoresis. Then, the forward primer ACTCCTACGG-GAGGCAGCA and reverse primer GGACTACHVGGGTWTCTAAT were used for PCR amplification of the V3-V4 hypervariable region. Low quality and repeated sequences as well as chimeric sequences were excluded, and the sequence with the length of 430 bp was obtained. The number of taxonomic ranks, and alpha- or beta- diversity of gut microbiota was analyzed in multiple dimensions, as well as the metabolic pathways predicted in different gut microbiota. Then, gutMGene database (<http://bio-annotation.cn/gutmgene/home.dhtml>) were searched to determine chemical components in LBRDDS which could directly regulate gut microbiota.

Network pharmacology analysis and molecular docking

The target genes by LBRDDS were predicted by SEA Search Server Database (<https://sea.bkslab.org/>) (Keiser et al., 2007). The target genes in depression were retrieved from GeneCards, OMIM, Disgenet, Therapeutic Target Database and other databases. The target genes by LBRDDS and target genes in depressions were matched to determine the overlapped ones. The overlapped genes were imported into the STRING database to find out the core genes using the CytoNCA plugin, and the obtained core target genes were subjected to gene ontology and KEGG pathway enrichment analysis. Cytoscape software was used to construct the regulatory network between the key components of LBRDDS and the target genes, and the components with higher ranking in the regulatory network map were selected and imported into Auto Dock Tool software for molecular docking, to identify the binding affinity of ligand and receptor components. Three-dimensional structures of protein were downloaded from Protein Data Bank (PDB) database (<https://www.rcsb.org/>), and three-dimensional structures of molecular ligands from ChemSpider database (<http://www.chemspider.com/>) were retrieved. Three-dimensional structures of proteins and ligands files were uploaded to the CB-Dock2 website (<https://cadd.labshare.cn/cb-dock2/php/example.php>) for auto blind docking (Liu et al., 2022; Yang et al., 2022b). The binding capacity of the ligand to the receptor was evaluated by energy matching. According to the degree of affinity between the component and the target gene, binding affinity was selected for visualization.

Extraction of primary cortical neurons and cell culture

SD rats were sacrificed on the 18th day of pregnancy, and the abdomen was opened. The heads of all fetal rats were separated from the bodies, and then skulls were removed. The intact brain tissue was placed in precooled PBS buffer, and then the cerebrovascular and meninges were removed one by one in precooled DMEM-F12 medium, and the prefrontal cortex tissue was isolated. The prefrontal tissue was cut into uniform pieces, added with 0.05 % trypsin and digested in a 37 °C cell incubator for 20 min, shaken once every 5 min. After termination of digestion, a 80-mesh sieve was used for filtration to obtain primary

prefrontal cortical neuron cell suspension. The cells were resuspended in DMEM-F12 medium after centrifugated at 1000 rpm for 5 min and seeded in 96-well plates. After 4 h, the medium was replaced with neurobasal medium, and half of the medium was changed every 3 days. After 7 days, the purity of primary cortical neurons was identified by immunofluorescence double staining with DAPI, tubulin and MAP2.

PC12 cells and Neuro-2a cells were purchased from Kunming Cell Bank, Chinese Academy of Sciences. The medium was added with 10 % fetal bovine serum +1 % penicillin/streptomycin solution. For the primary prefrontal cortical neurons, neurobasal serum-free complete medium was used added with glutamine 1 % +2 % penicillin/streptomycin +2 % B27 solution. Cells were cultured at 37 °C with 5 % CO₂. Cells in the logarithmic growth phase were applied in the experiment.

Construction of nerve cell injury model and drug administration

Firstly, the blank and drug-containing serum were tested for Neuro-2a cytotoxicity. The concentration range of serum was 5 %, 10 %, 15 %, 20 %, 30 %, 40 %, 50 %, and the serum with low cytotoxicity was selected for pharmacodynamic experiments. Primary cortical neurons, PC12 cells, and Neuro-2a cells were suspended at a concentration of 5 \times 10⁴/ml, and the number of cells in each well was 1 \times 10⁴. The cells were seeded in 96-well plates in quadruplicate and were divided into control group and CORT model group. In the control group, routine medium was used, and in the model group a complete medium containing CORT 100 μM , 200 μM , 400 μM , 600 μM , and 800 μM . Each well was added with CCK8 solution 24 h after seeding, and incubated in an incubator at 37 °C for 2 h. The optical density (OD) value at 450 nm was measured by a microplate reader to calculate the cell viability and the appropriate CORT concentration for the construction of cell models. Primary cortical neuronal cells, PC12 cells, and Neuro-2a cells were divided into control group (5 %, 10 %, 15 %, 20 % blank serum), CORT model group (5 %, 10 %, 15 %, 20 % blank serum CORT 400/600 μM), LBRDDS group (5 %, 10 %, 15 %, 20 % LBRDDS+CORT 400/600 μM). After 24 hours, 10 % CCK8 solution was added, and the cell viability was detected at OD 450 nm after 2 hours of culture at 37°C. 150 μl LDH release reagent was added to replace the original medium. After 1 h of culture at 37°C, the solution of each well was transferred to a new 96-well plate, and the LDH level was detected at OD 490 nm. The drug-containing serum concentration with the highest cell viability and the lowest LDH level was selected as the optimal pharmacological concentration to protect CORT-induced nerve cell damage for the next experiment.

Elisa detection of neurotransmitters and inflammatory factor levels

Cells were seeded into 96-well plates (1 \times 10⁴ cells/well) and divided into control group (5 %/10 % blank serum), CORT group (5 %/10 % blank serum+CORT 400 / 600 μM), LBRDDS group (5 %/10 % LBRDDS+CORT 400/600 μM). After incubation at 37°C for 24 h, the cell supernatant was collected for ELISA kits detection of neurotransmitters 5-hydroxytryptamine (5-HT), glutamate (Glu), GABA and inflammatory factors such as interleukin-1 β (IL-1 β) and interleukin-10 (IL-10). In each well 10 μl of sample were mixed with 40 μl of sample dilution, and were incubated at 37 °C for 30 min. The plate was washed 5 times, and in each well 50 μl of corresponding reagent was added. The plate was incubated at 37 °C for 30 min, and then washed 5 times. In each well, 50 μl of chromogenic agent A and B were added, and then were incubated at 37 °C for 10 min. Finally, 50 μl of termination solution was added and the absorbance at 450 nm was measured using a microplate reader. The sample concentration was calculated according to the OD value.

Cell transfection with miRNA silencing and overexpression

From Vigene Biosciences (WZ Biosciences Inc., Jinan, China), miR-144-3p overexpression and interference vector plasmids and their vehicle vector were purchased. Cells interventions experiments were

grouped as follows: CORT group (pAV-CMV-GFP-sh-NC plasmid+CORT), miRNA-144-3p inhibitor+CORT group (pAV-CMV-GFP-miR-144-3p interference plasmid+CORT), CORT+LBRD group (pAV-CMV-GFP-miRNA-OE-NC plasmid+CORT+LBRDDS), miR-144-3p OE+CORT+LBRDDS group (pAV-CMV-GFP-miR-144-3p overexpressed plasmid+CORT+LBRDDS). CORT-stimulated neurons were transfected with miR-144-3p overexpression, interference plasmids and corresponding NC plasmids. After plasmid transfection for 24 h, these cells were simultaneously incubated with CORT (600 μ M) and LBRDDS (10 %) for 24 h. Transfection was conducted using lipofectamine™ 3000.

Quantitative RT-PCR and western blotting

Total RNA was extracted from Neuro-2a cells according to the instructions of the cell-specific RNA extraction kit, and cDNA was obtained using the reverse transcription kit. According to the $2^{-\Delta\Delta C_t}$ method, amplification levels of the mRNAs and miRNAs relative to controls were computed. U6 and glyceraldehyde-3-phosphate dehydrogenase (GAPDH) were used as the endogenous control for the normalization of quantitative real-time PCR (qRT-PCR) data. Primer sequence information of the tested gene were listed in Supplementary Table 1. Neuro-2a cells were lysed with RIPA for 30 min and centrifuged at 12000 rpm for 10 min to obtain total protein supernatant. The protein concentration was measured and normalized, and the protein sample was obtained after heating at 100°C for 5 min. After electrophoresis, 10 μ g proteins were transferred onto nitrocellulose membranes (Millipore, Darmstadt, Germany). Then, the membrane was blocked with quick blocking solution at the room temperature for 15 min, and then incubated overnight with primary antibodies of glutamate decarboxylase 67 (Gad67) (ab26116, Abcam, Cambridge, UK, 1:2000 in dilution), vesicular GABA transporter (VGAT) (ab307448, Abcam, Cambridge, UK, 1:2000 in dilution), GAPDH (A3129, ABclonal Technology, Wuhan, China, 1:4000 in dilution). After incubations with their corresponding secondary antibodies conjugated with peroxidase (GB23303, Servicebio Biotechnology, Wuhan, China), these proteins were visualized by using the

enhanced chemiluminescence (ECL) plus immunoblotting detection system (Bio-Rad, California, US). The protein expression level of each strip was measured by Image-J software (National Institutes of Health), and normalized with the respective GAPDH.

Statistical analysis

All experiments were repeated at least in triplicate prior to statistical analysis and the results were expressed as mean \pm standard error of mean (SEM). Differences between two groups were compared by Student's *t*-test, while the comparison between three or more groups were performed through one-way analysis of variance (ANOVA). Differences were considered to be statistically significant at $p < 0.05$, with $p < 0.01$, and $p < 0.001$ considered highly statistically significant. Analysis and graphing were performed using GraphPad Prism 8.0 software (San Diego, CA, USA).

Results

Identification of the LBRD absorbed into blood by UHPLC-Q-TOF/MS

Different chemical components showed different peaks in different scanning modes, and our mass spectrometry analysis was performed using positive and negative ion mode scanning with a scanning range of *m/z* 100 to 1500. The data of high-resolution liquid collection were processed by CD3.3 (Thermo Fisher) and further with mzCloud (<https://www.mzcloud.org/>) and Natural Products (<https://coconut.naturalproducts.net/>) database, retain mzCloud best components of the comprehensive score greater than 60 points in the match. Total ion current profile of blank serum, LBRD and LBRDDS are shown in Fig. 1. The main chemical constituents of blank serum and LBRD were listed in the Supplementary Table 2-3. LBRD absorbed into blood components were shown in Supplementary Table 4. After de-duplication analysis, 33 components in LBRDDS were finally determined (Table 1), including palmitic acid, adrenic acid, linoleic acid, arachidonic acid, 11,12-

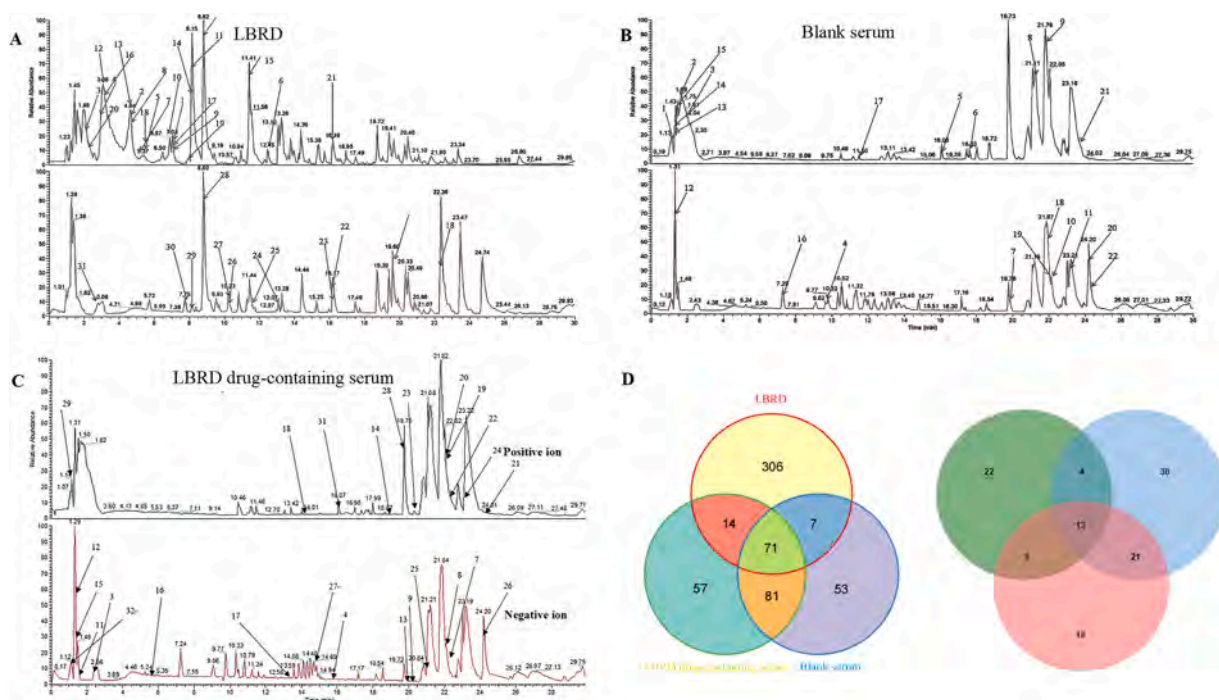


Fig. 1. Total ion flow map for natural product identification in LBRD, blank serum and LBRDDS samples. (A) Total ion flow map for natural product identification in LBRD. (B) Total ion flow map for natural product identification in blank serum. (C) Total ion flow map for natural product identification in LBRDDS. Column 1 is the total ion current diagram of negative ion mode, and column 2 is the total ion current diagram of positive ion mode. (D) Venn diagram of intersection of three sample active components: LBRD, blank serum and LBRDDS; LBRDDS intersection diagram of the active components of the three repeated tests.

Table 1Characterization of the chemical constituents in co-decoction of *L. henryi* Baker and *R. glutinosa* (Gaertn.) DC. containing serum by UPLCQTOF-MS/MS.

| Serial number | Name | Reference Ion | Formula | m/z | RT [min] |
|---------------|----------------------------------|---------------|---------------|-----------|----------|
| 1 | Hexanoylcarnitine | + | C13 H25 N O4 | 260.1856 | 9.278 |
| 2 | Flurandrenolide | + | C24 H33 F O6 | 414.24648 | 10.846 |
| 3 | Indole-3-lactic acid | - | C11 H11 N O3 | 204.0661 | 11.74 |
| 4 | 4-Phenylbutyric acid | + | C10 H12 O2 | 165.091 | 15.782 |
| 5 | Androsterone | + | C19 H30 O2 | 272.21391 | 17.159 |
| 6 | Progesterone | + | C21 H30 O2 | 314.22454 | 17.01 |
| 7 | Eicosapentaenoic acid | + | C20 H30 O2 | 309.242 | 22.262 |
| 8 | Hexadecanamide | + | C16 H33 N O | 256.2632 | 22.045 |
| 9 | Docosahexaenoic acid ethyl ester | + | C24 H36 O2 | 357.2782 | 19.995 |
| 10 | D- (+)-Tryptophan | + | C11 H12 N2 O2 | 204.08975 | 7.24 |
| 11 | L- (-)-Methionine | + | C5 H11 N O2 S | 150.0583 | 1.53 |
| 12 | DL-Arginine | + | C6 H14 N4 O2 | 175.1188 | 1.386 |
| 13 | 11,12-epoxyeicosenoic acid | + | C20 H32 O3 | 303.2311 | 19.769 |
| 14 | (±)9-HpODE | - | C18 H32 O4 | 311.2228 | 18.779 |
| 15 | L-Histidine | + | C6 H9 N3 O2 | 156.0768 | 1.418 |
| 16 | L-Phenylalanine | + | C9 H11 N O2 | 166.0862 | 5.715 |
| 17 | Isoquinoline | + | C9 H7 N | 130.0652 | 13.455 |
| 18 | Azelaic acid | - | C9 H16 O4 | 187.0968 | 14.059 |
| 19 | Linoleic acid | - | C18 H32 O2 | 279.2327 | 22.606 |
| 20 | Arachidonic acid | - | C20 H32 O2 | 303.2329 | 22.504 |
| 21 | Stearic acid | - | C18 H36 O2 | 283.2644 | 24.456 |
| 22 | Adrenic acid | - | C22 H36 O2 | 331.2643 | 22.975 |
| 23 | Deoxycholic acid | - | C24 H40 O4 | 391.2855 | 20.005 |
| 24 | Palmitic acid | - | C16 H32 O2 | 255.2327 | 23.085 |
| 25 | Docosahexaenoic acid | + | C22 H32 O2 | 329.247 | 20.949 |
| 26 | Docosapentaenoic acid | + | C22 H34 O2 | 331.2627 | 24.148 |
| 27 | 2-Amino-1,3,4-octadecanetriol | + | C18 H39 N O3 | 318.29999 | 14.836 |
| 28 | Testosterone Propionate | - | C22 H32 O3 | 343.22778 | 19.724 |
| 29 | methadone-d9 | - | C21H18D9NO | 316.94757 | 1.121 |
| 30 | Acetyl-L-carnitine | + | C9 H17 N O4 | 204.12308 | 1.779 |
| 31 | Thromboxane B2 | - | C20 H34 O6 | 369.22821 | 16.191 |
| 32 | 1-Methylnicotinamide | + | C7 H8 N2 O | 137.07094 | 1.202 |

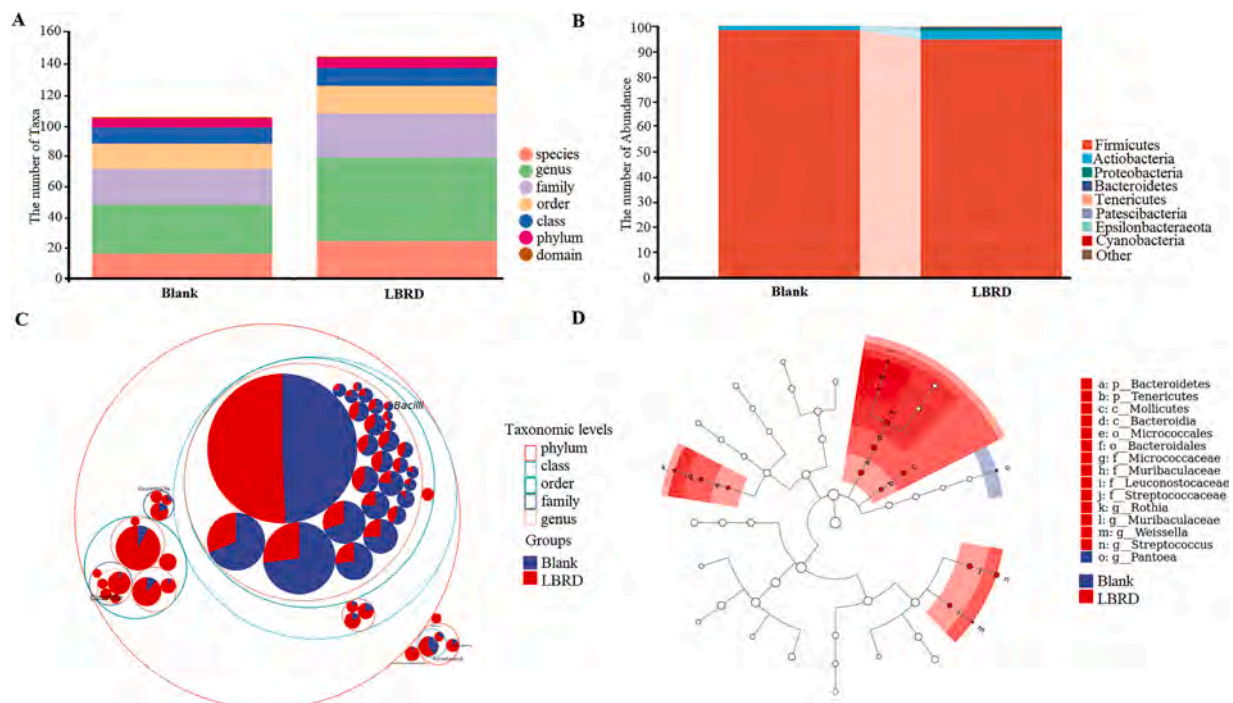


Fig. 2. LBRD regulates gut microbiota diversity and composition. (A) Gut microbiota taxon number statistics. (B) Gut microbiota taxonomic composition analysis. (C) Gut microbiota taxonomic level analysis. (D) Gut microbiota structure difference LEfSe analysis. It is shown that the taxonomic hierarchy of the main taxa in the sample community from phylum to genus (inner circle to outer circle). The node size corresponds to the average relative abundance of the taxon. Hollow nodes represent taxa that do not differ significantly between groups, while red nodes represent taxa that differ significantly between groups, with darker colors indicating more significant differences.

epoxyeicosenoic acid and other fatty acid endogenous metabolites, and various amino acid components such as tryptophan, phenylbutyric acid, l-phenylalanine, methionine and histidine, as well as other hormone components like androsterone, fluroxycortisone, progesterone and testosterone propionate.

By analyzing the changes of LBRD components before and after being absorbed into blood, we found that the quality marker components verbascoside, catalpol in LBRD and other compounds of Chinese medicinals reported in the literature were not detected. We speculate that the molecular weight of the prototype compound component is large and cannot be directly absorbed into the blood or through the brain blood barrier, and they might be in the intestine for further decomposition.

Bioactive compounds in LBRDDS absorbed from intestinal tract were transformed or metabolized by the gut microbiota

To investigate the effect of LBRD on the gut microbiota, we performed 16S rRNA sequencing analysis of cecal contents from SD rats. Firstly, the diversity of alpha flora was compared, and the results showed that there were differences in the diversity indexes of Chao1, Goods coverage, Faith pd and Observed species between the two groups (Supplementary Figure 3A). Compared with the blank control group, the gut microbiota structure and diversity of LBRD group were changed, and the differences between groups were mainly concentrated in family, genus and species, among which the abundance of *Firmicutes* was decreased, the abundances of *Actinobacteria*, *Proteobacteria*, *Bacteroidetes*, *Tenericutes* were increased (Fig. 2A-C). Then, the beta diversity according to LefSe analysis showed that *Bacteroidetes*, *Tenericutes*, *Mollicutes*, *Bacteroidia*, *Micorococcales*, *Bacteroidales*, *Micrococcaceae*, *Leuconostocaceae*, *Rothia* and *Weissella* in the LBRD group showed significant differences in their abundance compared with the blank control group (Fig. 2D). Subsequently, we conducted prediction analysis on the metabolic pathways of gut microbiota enrichment (Supplementary Figure 3B). The metabolic pathways are shown in Supplementary Table 5, including nucleoside and nucleotide biosynthesis, amino acid biosynthesis, fatty acid and lipid biosynthesis, carbohydrate degradation

biosynthesis, secondary metabolite biosynthesis, and etc.

The gutMGene database showed that only palmitic acid, deoxycholic acid, arachidonic acid, eicosapentaenoic acid, l-phenylalanine, l-histidine, tryptophan could be used to retrieve the gut microbiota that clearly regulated the metabolism of the active components. The name of gut microbiota, ID number of CHEBI database and other information are shown in Supplementary Table 6. The results of 16S rRNA sequencing analysis were observed and compared as well as the results of the bacteria community that can regulate the metabolism of active substances obtained from the gutMGene database. It was found by us that *Bacteroides fragilis*, *Bacteroides thetaiotaomicron* and other *Bacteroides* groups overlapped with each other, suggesting that LBRD might improve the metabolism and transformation function of gut microbiota by targeting and regulating *Bacteroides*, promote the metabolism of fatty acids and a variety of amino acids, and improve the function of the nervous system by regulating neurotransmitter and endogenous metabolism.

Network pharmacology analysis of LBRDDS components and target genes

A total of 1131 target genes of LBRDDS were predicted by SEA Search Server database and overlapped with depression target genes in GeneCards, OMIM, Disgenet, Treatment Target Database and Genecard database. Finally, 108 core genes were obtained by adding RNA-seq gene. Network regulation map between 33 LBRDDS material components and 108 target genes (Fig. 3A). The outer circle represents the genes with degree ≤ 8 , the inner circle represents the genes with degree ≥ 9 , and the middle diamond part represents the key compound components of LBRDDS. The larger the diamond is, the more target genes can be enriched, indicating the degree of relationship with depression. According to network analysis, the genes with the highest degree value were FABP3, MAPK3, RELA, AKT1, FAAH and EPHX2. The core components were palmitic acid, adrenic acid, linoleic acid, arachidonic acid, 11,12-epoxyeicosenoic acid, docosapentaenoic acid and 4-phenylbutyric acid. Gene ontology analysis consists of three parts, biological process, cellular component and molecular function, which respectively represent the biological process, molecular function and cellular

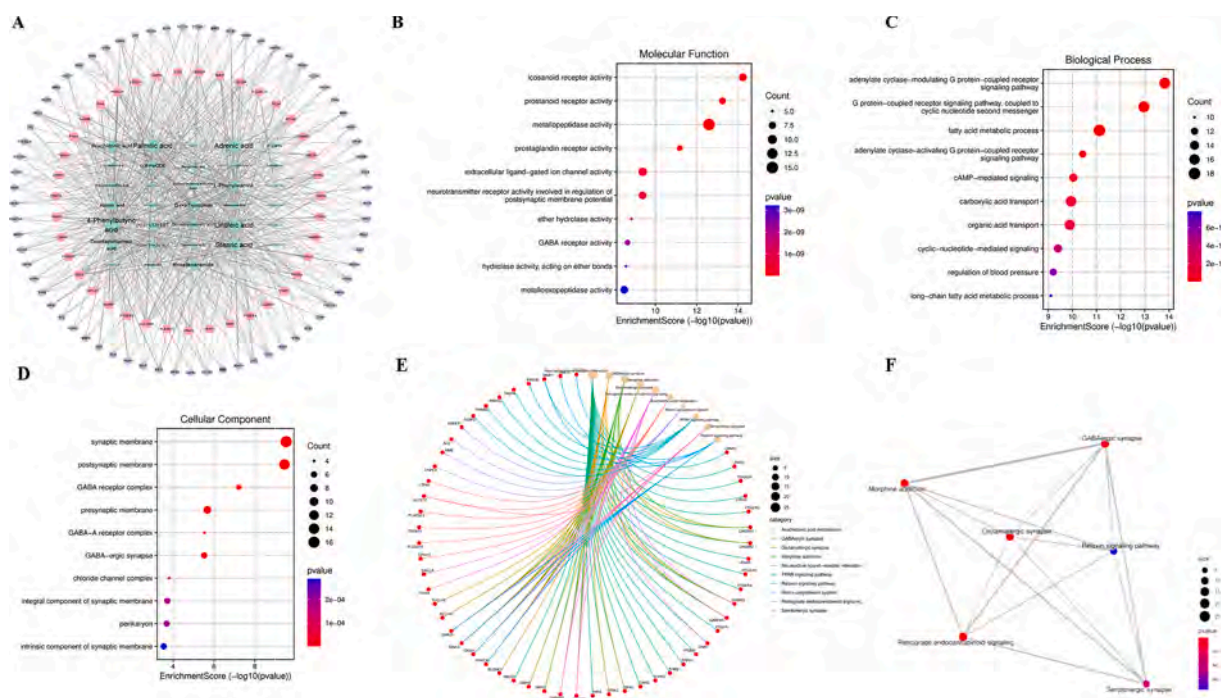


Fig. 3. Network pharmacology analysis of LBRDDS components and target genes. (A) Regulatory network of key active components of LBRDDS and core target genes. (B-D) Gene ontology analysis of core target genes MF, BP, CC. (E) KEGG pathway enrichment analysis of core target genes. (F) KEGG pathway interaction network map.

localization. Biological process (Fig. 3B) involved fatty acid metabolic process, cAMP-mediated signaling, carboxylic acid transport, organic acid transport, long-chain fatty acid metabolic process. Cellular component (Fig. 3C) involved synaptic membrane, GABA receptor complex, presynaptic membrane, GABA-A receptor complex, GABAergic synapse. Molecular function (Fig. 3D) involved metalloproteinase activity, prostaglandin receptor activity, neurotransmitter receptor activity, GABA receptor activity, metalloproteinase activity. The KEGG enrichment pathways of key target genes and the correlation between pathways are shown in Fig. 3E-F. GABAergic synapse, glutamatergic synapse and serotonergic synapse pathways are closely related and can regulate each other.

Gene ontology biological process analysis indicated fatty acid metabolic process and GABA receptor activity were involved and KEGG enrichment pathway indicated that neuroactive ligand-receptor interaction, GABAergic and glutamatergic synapse, and arachidonic acid metabolism were involved. Such results showed that the active components of LBRD in the blood mainly regulated fatty acid metabolism, restored the balance between the synaptic plasticity of excitatory glutamatergic neurons and the synaptic plasticity of inhibitory GABAergic neurons, enhanced neuronal function and signal transduction, reversed nerve cell damage induced by CORT, and played a neuroprotective role. Multiple pathways were closely related and mutually regulated, indicating that LBRD could regulate multiple targets and multiple pathways and had a strong regulatory effect on the nervous system.

Molecular docking of LBRDDS components and target genes

Molecular docking is a theoretical simulation method to predict the binding mode and affinity of a drug from the characteristics of the receptor and the interaction between the receptor and the drug molecule. Finally, serum metabolites such as palmitic acid, adrenic acid, linoleic acid, arachidonic acid, 11,12-epoxyeicosenoic acid, docosapentaenoic acid and key depression target genes *FABP3* (3WBG), *MAPK3* (4QTB), *RELA* (1VJ7), *AKT1*(7FCV), *FAAH* (3QJ8), *EPHX2* (5ALF) were selected and imported into CB-Dock2 for molecular docking. The docking process was conducted in triplicate, as shown in Table 2. At the same time, the docking results were analyzed by heat map clustering analysis, and the results with higher binding affinity were selected to generate visual images in the CB-Dock2 system and export them. The molecular docking visualization pictures of FAAH with adrenic acid, FAAH with linoleic acid, FAAH with arachidonic acid, FAAH with 11,12-epoxyeicosenoic acid, FAAH with docosapentaenoic acid, EPHX2 with 11,12-epoxyeicosenoic acid are shown in Fig. 4A-F. The lower the binding energy, the higher the binding affinity, and the easier ligand is to bind to the receptor components. Heat map clustering analysis of molecular docking results is shown in Fig. 4G. Heat map clustering analysis of molecular docking results showed that FAAH had the lowest binding energy with multiple components, indicating that it had the strongest binding affinity. Therefore, FAAH might be the most important target gene in regulating gut microbiota and metabolic function. In order to verify the predicted target genes of molecular docking, we used qRT-PCR to detect the expression of FAAH and EPHX2 in Neuro-2a cells of CORT 600 μ M group and 10 % LBRDDS group. The results showed that the expression levels of FAAH and EPHX2 in the LBRDDS group were significantly

decreased with comparison of CORT treated group ($p < 0.001$, Fig. 4H). The above results indicate that FAAH and EPHX2 play an important role in the neuroprotection of LBRDDS.

Protective effect of LBRDDS on nerve cell injury models

Compared with control cells, blank serum (5 %, 10 %, 15 %) had no significant effect on cell viability. 20 % blank serum cell survival rate was significantly decreased to 72 % ($p < 0.001$). 20 % drug-containing serum cell survival rate was significantly decreased ($p < 0.01$). As the concentration of drug-containing serum increased, the cell survival rate gradually decreased in a concentration-dependent manner. Therefore, concentrations within 20 % were selected for pharmacodynamic screening in subsequent experiments (Supplementary Figure 4). The immunofluorescence double-stain identification of primary cortical neurons was followed by DAPI, tubulin, and MAP2 staining and the images were merged (Fig. 5A). The results showed that the isolation and culture of primary cortical neurons could be used for the subsequent experimental study. Twenty-four hours after treated with CORT of 100 μ M, 200 μ M, 400 μ M, 600 μ M, and 800 μ M, the survival rate of primary cortical neurons, PC12 and Neuro-2a cells decreased to various degrees. The cell viability of primary cortical neurons and PC12 cells (CORT 400 μ M) and Neuro-2a cells (CORT 600 μ M) was significantly decreased to about 50 % ($p < 0.001$, Fig. 5B and Fig. 6A, D). Therefore, CORT 400 μ M was determined as the intervention concentration of primary cortical neurons and PC12 cells cell model, and CORT 600 μ M was determined as the action concentration of Neuro-2a cells model for subsequent cell experiments. Next, the protective effects of different concentrations of LBRDDS on cell viability and LDH cytotoxicity in depression cell model were tested. The results showed that compared with the control group, the cell survival rate of the model group was significantly decreased ($p < 0.001$). Compared with the model group, 5 % LBRDDS could significantly increase the survival rate of primary cortical neurons ($p < 0.01$), and 10 % LBRDDS could significantly increase the survival rate of PC12 cells and Neuro-2a cells ($p < 0.01$, $p < 0.001$; Fig. 5C and Fig. 6B, E). Meanwhile, compared with the control group, LDH cytotoxicity in model group was significantly increased ($p < 0.05$, $p < 0.01$). Compared with model group, LDH cytotoxicity in LBRDDS group was significantly reduced ($p < 0.01$; Fig. 5D and Fig. 6C, F). LDH level is an important indicator of cell membrane integrity, and quantitative analysis of cytotoxicity can be achieved by detecting the level of LDH released into culture from cells with ruptured plasma membrane. The primary cortical neurons cell pattern image of control, CORT 400 μ M, 5 % LBRDDS is shown in Fig. 5E-G. The PC12 cell pattern image of control, CORT 400 μ M, 10 % LBRDDS is shown in Fig. 6G-I. The Neuro-2a cells mode image of control, CORT 600 μ M, LBRDDS (10 %) is shown in Fig. 6J-L. These results indicated that nerve cell survival rate significantly decreased and LDH cytotoxicity increased after CORT 400 or 600 μ M treatment, while 5 % or 10 % LBRDDS could increase nerve cell survival rate, protect cell integrity, decrease LDH cytotoxicity, reduce nerve cell death and relieve cell injury.

Effects of LBRDDS on neurotransmitters and inflammatory cytokines

The results on primary neuron cells are shown in Fig. 7A-E.

Table 2
Depression core target genes and components of molecular docking results (kJ/mol)

| Component name PDB ID | FABP3 (3WBG) | MAPK3 (4QTB) | RELA (1VJ7) | AKT1 (7FCV) | FAAH (3QJ8) | EPHX2 (5ALF) |
|----------------------------|-----------------|-----------------|----------------|----------------|----------------|-----------------|
| Palmitic acid | -4.85±0.06 | -4.27±0.31 | -4.53±0.31 | -4.73±0.31 | -4.77±0.31 | -5.8±0.12 |
| Adrenic acid | -5.93±0.26 | -4.63±0.06 | -5.2±0.11 | -5.9±0.42 | -6.34±0.21 | -5.35±0.51 |
| linoleic acid | -5.5±0.22 | -4.4±0.1 | -5.2±0.2 | -5.23±0.59 | -6.47±0.36 | -5.73±0.63 |
| Arachidonic acid | -5.88±0.19 | -4.77±0.23 | -5.3±0.36 | -5.83±0.22 | -6.57±1.25 | -5.73±0.88 |
| 11,12-epoxyeicosenoic acid | -5.63±0.15 | -4.87±0.12 | -5.77±0.38 | -6.23±0.22 | -6.33±1.27 | -6.48±0.21 |
| Docosapentaenoic acid | -6.05±0.21 | -4.87±0.23 | -5.57±0.4 | -6.13±0.67 | -6.37±1.24 | -6.13±0.59 |

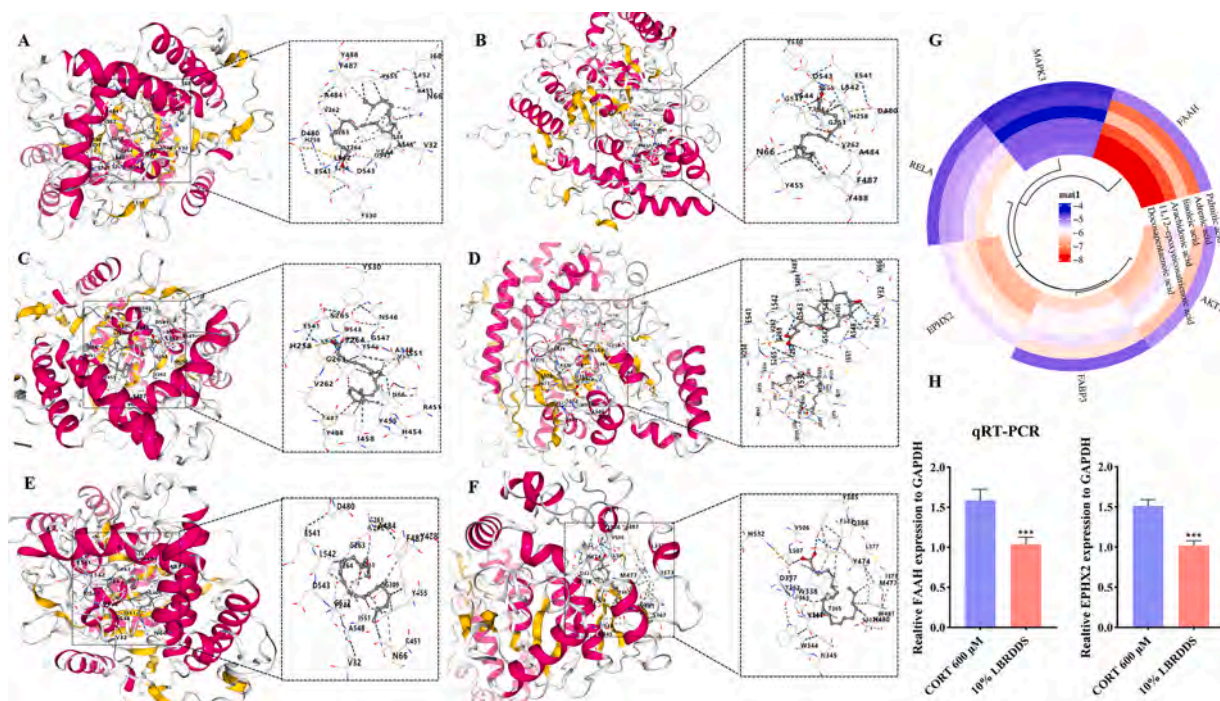


Fig. 4. Molecular docking of LBRDDS core components and target genes. (A) FAAH (3QJ8) and adrenic acid. (B) FAAH (3QJ8) and linoleic acid. (C) FAAH (3QJ8) and arachidonic acid. (D) FAAH (3QJ8) and 11,12-epoxyicosenoic acid. (E) FAAH (3QJ8) and docosapentaenoic acid. (F) EPHX2 (5ALF) and 11,12-epoxyicosenoic acid. The lower the binding energy, the higher the binding affinity, and the easier the compound is to bind to the target gene. (G) Heat map clustering analysis of molecular docking results. (H) Relative FAAH and EPHX2 expression to GAPDH in Neuro-2a cell. Data are expressed as mean \pm SEM. *** $p < 0.001$, compared with the CORT group.

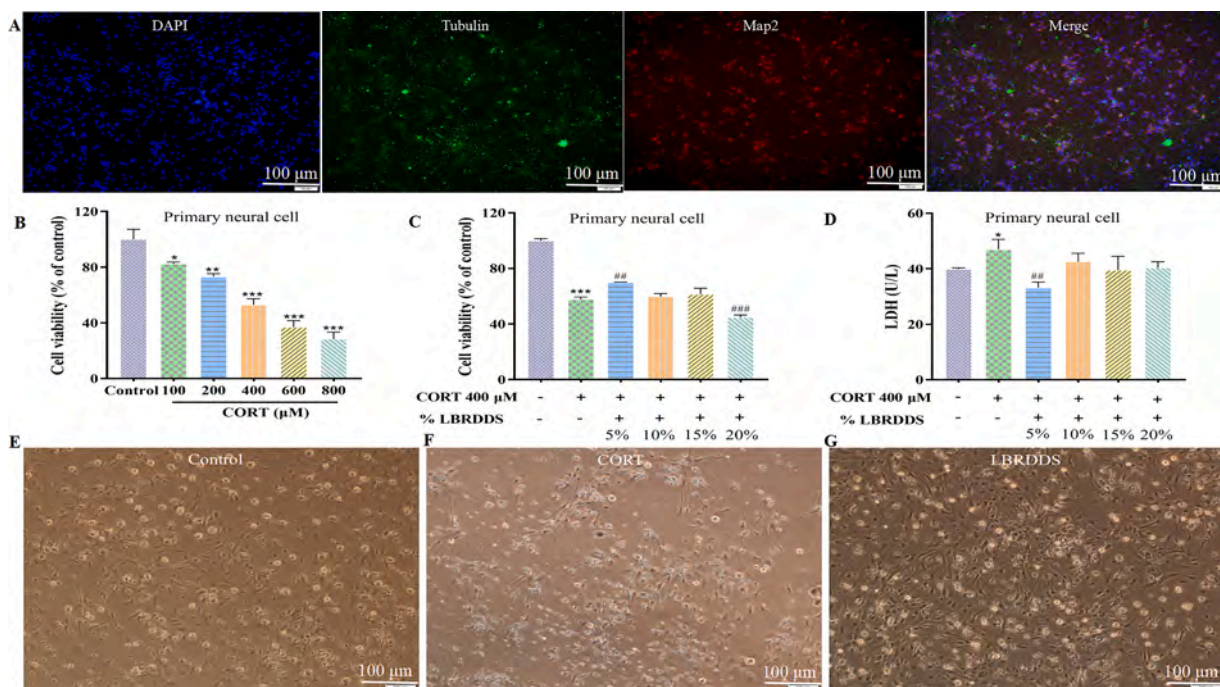


Fig. 5. Effect of LBRDDS on the vitality of CORT-induced primary cortical neurons cell injury model. (A) The immunofluorescence double-stain identification of primary cortical neurons was followed by DAPI, Tubulin, MAP2 and Merged staining. (B) The cell vitality of primary neurons after CORT injury at different concentrations were measured by CCK8 assay (C) Effect of 5 %, 10 %, 15 %, 20 % concentrations LBRDDS on CORT-induced primary neuron cell activity were measured by CCK8 assay; (D) Effect of 5 %, 10 %, 15 %, 20 % concentrations LBRDDS on CORT-induced primary neuron cell were assessed by LDH enzyme activity. (E-G) Schematic diagram of primary neuron cell vitality in control, CORT and 5 % LBRDDS groups. Data are expressed as mean \pm SEM. Compared with the control group, * $p < 0.05$, ** $p < 0.01$, *** $p < 0.001$, respectively; compared with the CORT (400 μ M), ## $p < 0.01$, ### $p < 0.001$, respectively.

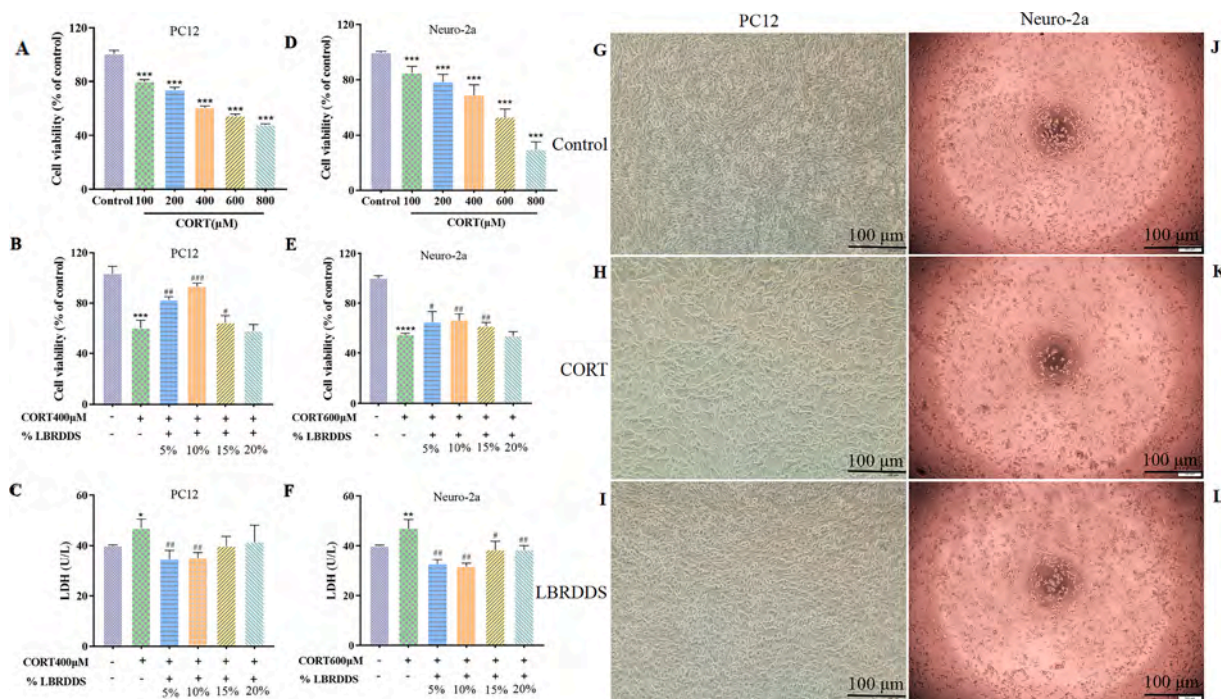


Fig. 6. Effect of LBRDDS on the vitality of CORT-induced PC12 and Neuro-2a cells injure model. (A) The PC12 cell vitality treated with CORT at different concentrations was evaluated by CCK8 assay. (B) Effect of 5%, 10%, 15%, 20% concentrations LBRDDS on CORT-induced PC12 cell was tested by CCK8 assay. (C) Effect of 5%, 10%, 15%, 20% concentrations LBRDDS on CORT-induced PC12 cell was assessed by LDH enzyme activity. (D) The Neuro-2a cells vitality treated with CORT at different concentrations was evaluated by CCK8 assay. (E) Effect of 5%, 10%, 15%, 20% concentrations LBRDDS on CORT-induced Neuro-2a cells was evaluated by CCK8 assay. (F) Effect of 5%, 10%, 15%, 20% concentrations LBRDDS on CORT-induced Neuro-2a cells was assessed LDH enzyme activity. (G-I) Schematic diagram of PC12 cell vitality in control, CORT 400 μM and 10% LBRDDS groups. (J-L) Schematic diagram of Neuro-2a cell vitality in control, CORT 600 μM and 10% LBRDDS groups. Data are expressed as mean ± SEM. Compared with the control group, **p* < 0.05, ***p* < 0.01, ****p* < 0.001, respectively; compared with the CORT group, #*p* < 0.05, ##*p* < 0.01, ###*p* < 0.001, respectively.

Compared with the control group, the expression levels of 5-HT, GABA and IL-10 in the model group (CORT 400 μM) were significantly decreased, while the expression levels of Glu and IL-1β were significantly increased (*p* < 0.05, *p* < 0.01). On the contrary, compared with the model group, 5% LBRDDS significantly increased the expression levels of 5-HT, GABA and IL-10, and significantly decreased the expression levels of Glu and IL-1β (*p* < 0.05, *p* < 0.01, *p* < 0.001). The results on PC12 cells are shown in Fig. 7F-J. Compared with the control group, the expression levels of 5-HT, GABA, and IL-10 in the model group (CORT 400 μM) were significantly decreased, and the expression levels of Glu and IL-1β were significantly increased (*p* < 0.001). On the contrary, compared with the model group, the 10% LBRDDS significantly increased the expression levels of 5-HT, GABA and IL-10, and significantly decreased the levels of Glu and IL-1β (*p* < 0.05, *p* < 0.01, *p* < 0.001, respectively). The results on Neuro-2a cells are shown in Fig. 7K-O. Compared with the control group, the expression levels of 5-HT, GABA and IL-10 in the model group (CORT 600 μM) were significantly decreased, and the expression levels of Glu and IL-1β were significantly increased (*p* < 0.05, *p* < 0.01). On the contrary, compared with the model group, the expression levels of 5-HT, GABA and IL-10 in the 10% LBRDDS group were significantly increased, while the expression levels of Glu and IL-1β were significantly decreased (*p* < 0.05, *p* < 0.01). These results suggested that CORT intervention could induce depression-like phenotypes in neurons, leading to E/I imbalance and elevated inflammation levels, while LBRDDS could reverse the levels of neurotransmitters and inflammatory cytokines, and protect neurons cells from CORT-damaged, showing a good neuroprotective effect. In addition, we also selected the optimal concentration of Mifepristone (2.5 μM) (CORT receptor antagonist, also known as RU486) as a positive control drug to detect its pharmacological effects on the Neuro-2a cell model (CORT 600 μM). Compare with the CORT600 model group, the

levels of 5-HT, Glu and IL-10 were significantly improved, while the improvement of GABA and IL-1β was not statistically significant (Supplementary Figure 5). The pharmacological effect of LBRDDS was consistent with that of RU486, which proved that LBRDDS had a good neuroprotective effect.

LBRDDS regulate miRNA-144-3p expression mediated GABA synthesis and transport

In order to investigate the molecular mechanism of the effect of LBRDDS on GABA levels in nerve cell injury models, qRT-PCR and western blotting were used to analyze the expression levels of genes and proteins associated with GABA synthesis (Gad67) and release (VGAT). As shown in (Fig. 8A-C), CORT 600 μM intervention in Neuro-2a cells resulted in increased expression of miRNA-144-3p and decreased the expression level of *Gad67* and *VGAT* gene, while 10% LBRDDS significantly reversed these changes. Protein expression was consistent with qRT-PCR results, and 10% LBRDDS significantly increased the expression levels of *Gad-67* and *VGAT* proteins in the cell model (Fig. 8D-F); The pattern plot of the protein band in Fig. 8D is derived from the whole un-cropped images of the original western blots in the Supplementary Figure 6). The fluorescence intensity of GFP 48 h after plasmid transfection proved that the transfection experiment was successful (Fig. 8G), and qRT-PCR results showed that compared with CORT 600 μM group, miRNA-144-3p inhibitor + CORT 600 μM group and CORT 600 μM + 10% LBRDDS group miRNA-144-3p expression decreased, while *Gad67* and *VGAT* expression increased. Compared with CORT 600 μM + 10% LBRDDS group, the miRNA-144-3p expression levels in miRNA-144-3p OE + CORT 600 μM + 10% LBRDDS group were significantly increased, while the expression levels of *Gad67* and *VGAT* were significantly decreased (*p* < 0.001; Fig. 8H-J). The level of GABA was

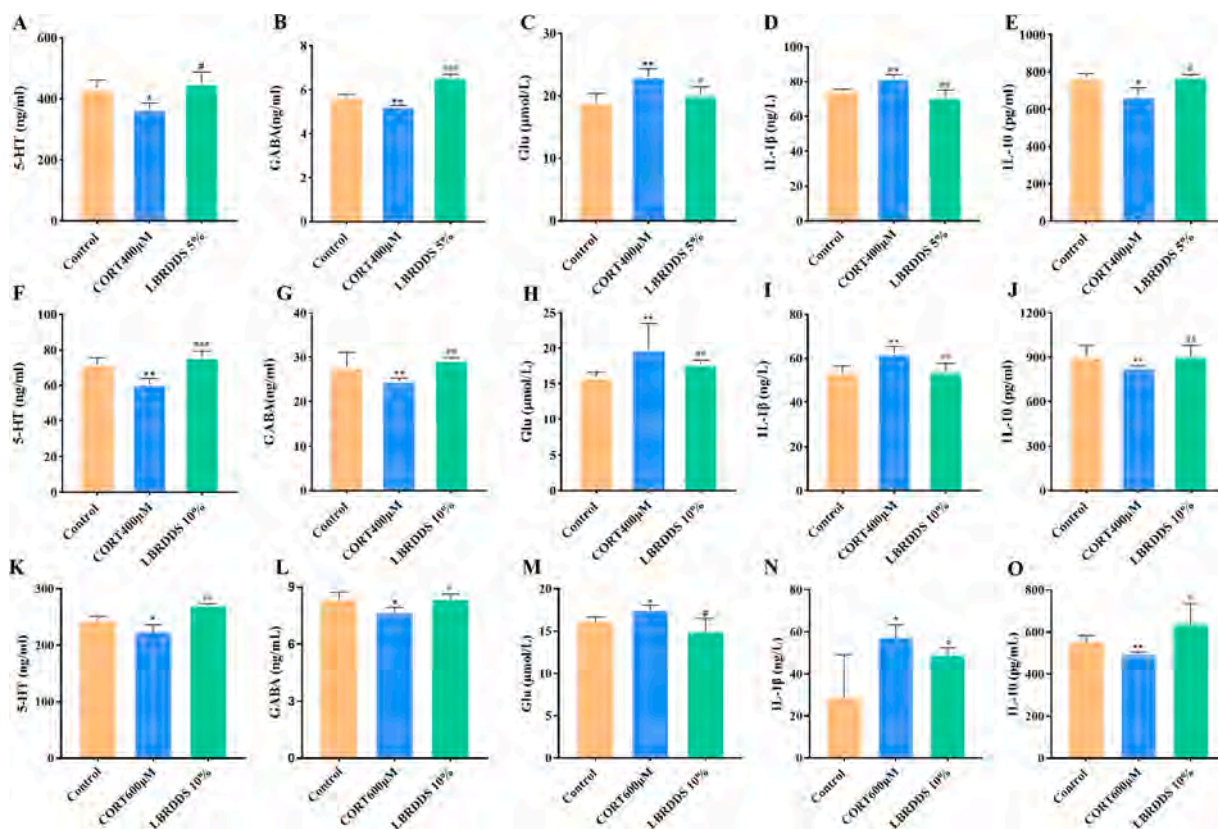


Fig. 7. Effects of LBRDDS on neurotransmitters and inflammatory cytokines of CORT-induced cell injury model. (A-E) Effect of 5% LBRDDS on 5-HT, GABA, Glu, IL-1 β , IL-10 levels in primary neuronal cell injury model induced by CORT (400 μ M). (F-J) Effect of 10% LBRDDS on 5-HT, GABA, Glu, IL-1 β , IL-10 levels in PC12 cell injury model induced by CORT (400 μ M). (K-O) Effect of 10% LBRDDS on 5-HT, GABA, Glu, IL-1 β , IL-10 levels in primary neuronal cell injury model induced by CORT (600 μ M). Concentration data are expressed as mean \pm SEM. Compared with the control group, * p < 0.05, ** p < 0.01, respectively; Compared with the CORT group, # p < 0.05, ## p < 0.01, ### p < 0.001, respectively.

consistent with the results of qRT-PCR. Compared with CORT 600 μ M + 10% LBRDDS group, the miRNA-144-3p expression levels in miRNA-144-3p OE + CORT 600 μ M + 10% significantly increased in LBRDDS group, while the expression levels of *Gad67* and *VGAT* were significantly decreased (p < 0.001) (Fig. 8H-J). These results indicated that miRNA-144-3p could target and negatively regulate the expression of *Gad67* and *VGAT* genes. By regulating miRNA-144-3p mediated GABA synthesis and transport function, 10% LBRDDS could increase GABA concentration, and therefore it could relieve nerve cell damage caused by CORT so as to play an antidepressant role.

Discussion

Chinese medicinals have the advantages of multi-target, multi-approach and overall regulation in the treatment of depression, which has been widely recognized by all walks of life, and therefore there is a good prospect for developing new drugs originating from Chinese medicinals (Ma et al., 2020; Zheng et al., 2020). The underlying mechanism of LBRD working on depression and improving nervous system function might involve improving synaptic plasticity of GABAergic and glutamergic neurons, inhibiting the hyperactivation of inflammatory response, and increasing neurotrophic pathway signal transduction (Miao et al., 2019; Xue et al., 2022; Zhang et al., 2020). However, due to the unclear material basis of drug-containing serum and the controversial construction of depression cell model, the application of LBRD *in vitro* cell experiments is with limitations.

Therefore, we applied UHPLC-Q-TOF/MS to detect the active components in LBRDDS, and then analyzed gut microbiota regulated by LBRD using 16S rRNA technology, to predict the metabolic pathways that the gut microbiota involved, and to search the gut microbiota

suitable for the metabolism of the active components of LBRDDS. Subsequently, gene ontology and KEGG pathway enrichment analysis were performed on the target genes, and the regulatory network of LBRDDS key active components and depression target genes was constructed by network pharmacology technology, and the core target genes and components in the regulatory network were selected for molecular docking to verify the binding affinity between the components and target genes. According to the results of our study, it was concluded that the active component of LBRD absorbed into serum could change the abundance of gut microbiota by regulating the expression of key target genes, intervene the metabolic process of gut microbiota, reduce inflammatory response, and promote neurotransmitter synthesis pathway, which might be a key pathway for LBRDDS to play a neuroprotective role.

Primary cortical neuron cells and two neuronal cell lines damaged by CORT are used to construct an *in vitro* cell model to simulate the E/I imbalance and inflammatory damage of pathological mechanism of depression. The levels of neurotransmitters and inflammatory factors, 5-HT, GABA, Glu, IL-10 and IL-1 β , are detected to evaluate the establishment of the cell model and the protective effect of LBRDDS on CORT-induced cell injury model. In the previous research by us, luciferase reporter assay, RNA immunoprecipitation and RNA pull down assay were applied to obtain miRNA and mRNA regulatory networks. It was found that miRNA-144-3p could negatively regulate the expression of *Gad67* and *VGAT* mRNAs, improve the function of GABA neurons, and have significant antidepressant activity. Therefore, firstly, qRT-PCR and western blotting were used to verify the antidepressant effect of LBRDDS in enhancing GABA synthesis and transport by inhibiting miRNA-144-3p expression. Secondly, by transfecting miRNA-144-3p with low expression, overexpression and blank control vector, it was further verified

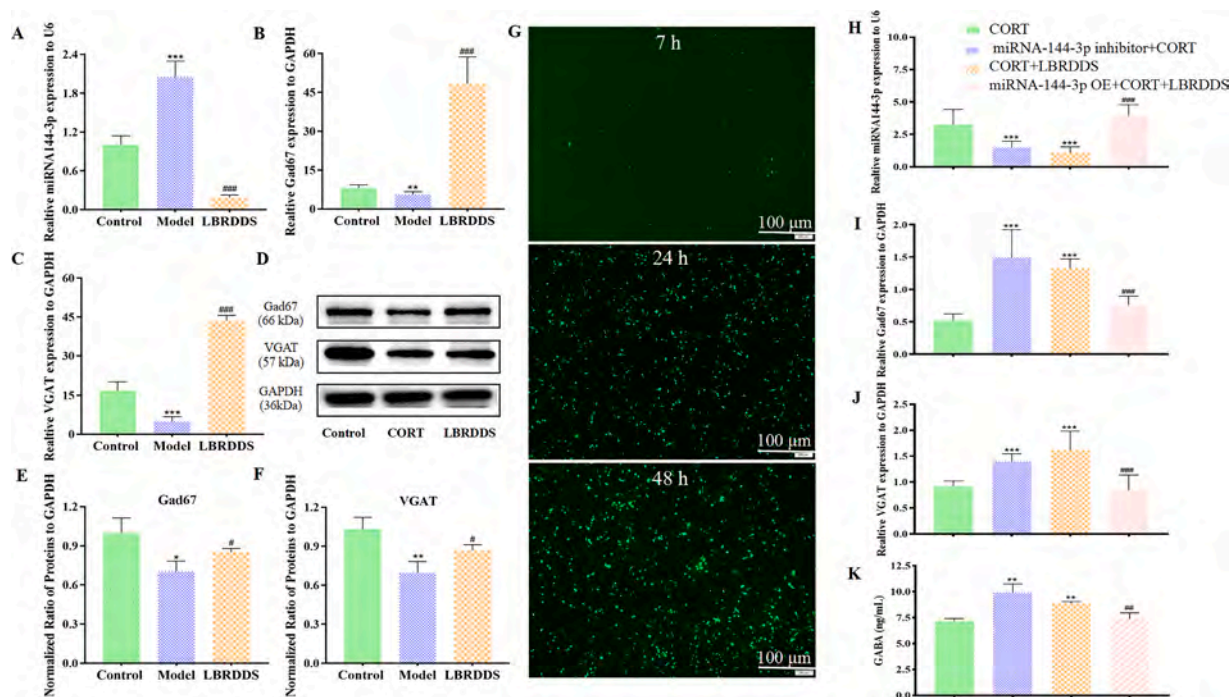


Fig. 8. LBRDDS rescued E/I imbalance via miRNA-144-3p mediated GABA synthesis, transport and release. (A–C) Effect of 10 % LBRDDS on miRNA-144-3p, *Gad67*/VGAT mRNAs expression in Neuro-2a cell injury model induced by CORT (600 μ M). U6 and GAPDH were set as the endogenous control. (D–F) Effect of 10 % LBRDDS on *Gad67* and VGAT protein expression in Neuro-2a cell injury model induced by CORT (600 μ M). Data are expressed as mean \pm SEM. Compared with the control group, * p < 0.05, ** p < 0.01, *** p < 0.001, respectively; compared with the CORT group, # p < 0.05, ### p < 0.001, respectively. (G) Schematic diagram of plasmid transfection efficiency with GFP fluorescence in 7 h, 24 h, 48 h. (H–K) Effect of altered miRNA-144-3p expression on the mRNAs of *Gad67*, VGAT and GABA levels in CORT-induced Neuro-2a cell injury model. Compared with the CORT group, ** p < 0.01, *** p < 0.001; Compared with the CORT+LBRDDS group, ## p < 0.01, ### p < 0.001. CORT group (pAV-CMV-GFP-sh-NC plasmid+CORT), miRNA-144-3p inhibitor+CORT group (pAV-CMV-GFP-miR-144-3p interference plasmid+CORT), CORT+LBRD group (pAV-CMV-GFP-miRNA-OE-NC plasmid+CORT+LBRDDS), miR-144-3p OE+CORT+LBRDDS group (pAV-CMV-GFP-miR-144-3p overexpressed plasmid+CORT+LBRDDS).

that perturbation of miRNA-144-3p expression could interfere with the antidepressant effect of LBRDDS.

With the continuous development and progress of TCM, a large number of clinical and experimental studies have shown that TCM formulas or Chinese medicinals have good clinical effect in the treatment of depression. LBRD, an important TCM formula, mainly plays an antidepressant role by increasing the secretion of neurotransmitter, inhibiting the level of inflammation in the body, and increasing the GABAergic neuron function and synaptic plasticity. At present, studies on the antidepressant effects of Chinese medicinals mainly focus on animal experiments *in vivo*, while there are few researches on cell experiments, for the pharmacodynamic material basis of drug-containing serum is unclear. Also, the metabolic process and mechanism of drug-containing serum *in vivo* are relatively complex. The effects by Chinese medicinals are usually affected by the dose, preparation, production area, and seasons, etc., and currently there are no unified quality control standards for the pharmacodynamic research of the active components in Chinese medicinals. After oral administration of Chinese medicinals, the metabolic process and pharmacokinetics of Chinese medicinals *in vivo* are the key links that affect the pharmacodynamic mechanism of drug containing serum. However, the active components of Chinese medicinals interact with each other, and the distribution, absorption and metabolism of different active components are different after entering the blood. In addition, they are also affected by factors such as the permeability of the blood-brain barrier to the pharmaceutical components. The active components of Chinese medicinals may interact with some components of the blood and then be converted into metabolites. The specific conversion process is still unclear, which makes the pharmacodynamic mechanism of drug-containing serum more complicated. Therefore, we applied UHPLC-Q-TOF/MS to analyze and identify the components of LBRD drug-containing serum. The results showed

that LBRDDS mainly contained two categories of components. One category mainly included fatty acid components such as arachidonic acid, palmitic acid, epoxyeicosaenoic acid, docosahexaenoic acid and so on. Another category mainly included tryptophan, l-phenylalanine, methionine, histidine and other amino acid components. Literature studies have shown that the brain is rich in unsaturated fatty acids, and some fatty acids belong to the family of lipid signaling mediators. Among them, arachidonic acid could mediate chronic inflammation of the central nervous system, damage the function of the nervous system, and play an important role in depression, anxiety, Alzheimer's disease and other nervous system diseases (Gorica and Calderone, 2022; Larrieu and Laye, 2018; Regulska et al., 2021). At present, relevant studies have confirmed that regulating the degradation and metabolism of epoxy fatty acids such as epoxyeicosatrienoic acid, epicosatetraenoic acid and eicosapentaenoic acid could effectively reduce inflammation and exert neuroprotective effects (Shan and Hashimoto, 2022). In addition, many studies have shown that fatty acids are closely related to depression, and improving the metabolic function of fatty acids can play a role in the treatment of depression (Grosso et al., 2014; Hsu et al., 2018). Tryptophan is an important precursor for the synthesis of neurotransmitter 5-HT, which plays an important role in the synthesis of neurotransmitters. In addition, most amino acids could maintain normal metabolism, enhance immunity, and improve nervous system function (Brown et al., 2022).

According to 16S rRNA results, for the first time it was demonstrated that the abundance and distribution structure of *Bacteroidetes*, *Leuconostocaceae*, *Weissella* and *Lactobacillus* in gut microbiota changed significantly after oral administration of LBRD. Both *Leuconostocaceae* and *Weissella* are *Lactobacillus*, and current studies have shown that *Leuconostocaceae* and *Weissella* are probiotics with clinical application potential, and have significant advantages in promoting apoptosis of

cancer cells and inhibiting inflammatory response (Ahmed et al., 2022; Zununi Vahed et al., 2017). A randomized, double-blinded, controlled trial showed that transplant of *Lactobacillus* could effectively prevent or relieve depression scale scores and clinical symptoms in patients with postpartum depression (Slykerman et al., 2017). In addition, other studies have shown that transplant of *Lactobacillus* could effectively reduce the concentration of canine and improve cognitive dysfunction in patients with severe depression (Rudzki et al., 2019). Further studies showed that *Lactobacillus* could increase GABA secretion, regulate vagus nerve function, increase GABA receptor expression, enhance GABA neuronal function, inhibit HPA axis overactivation, and improve depressive mood in mice model, and therefore *Lactobacillus* had a significant antidepressant effect (Bravo et al., 2011; Tette et al., 2022). The 16S rRNA analysis results and gutMGene database showed that *Bacteroides* might be another core microbiota regulated by LBRD, and *Bacteroides* could target and regulate the metabolism of arachidonic acid. At present, it has been reported that *Bacteroides* could directly regulate the metabolism of arachidonic acid, reduce intestinal permeability, reduce the level of corticosterone in intestinal tract and relieve the level of inflammation (Park et al., 2016). The relative abundance of *Bacteroides* is negatively correlated with the brain characteristics related to depression. *Bacteroides* could produce a large amount of GABA, which is considered to be a promising bacterium for the treatment of major depression (Strandwitz et al., 2019; Zhang et al., 2022b). *Bacteroides* could improve the metabolic system diseases such as obesity and diabetes and reduce inflammation by regulating the metabolism of fatty acids (Cani et al., 2008). We predicted that the metabolic pathways of different gut microbiota might be regulated by LBRD, and results by us showed that gut microbiota could regulate various endogenous metabolic pathways such as fatty acid and lipid anabolism, amino acid anabolism, carbohydrate synthesis and degradation, etc. This conclusion has been supported by other study. *Lactobacillus* and *Bacteroides* could treat neurological diseases by regulating metabolic pathways such as endogenous fatty acids (Chen et al., 2019; Xiao et al., 2022). Therefore, it is concluded that LBRD into blood active components could increase the abundance of *Bacteroides* and *Lactobacillus*, regulate the various metabolic pathways of gut microbiota, increase GABA secretion, improve the nervous system function and play a neuroprotective role.

KEGG and gene ontology analyses showed that LBRDDS target gene mainly regulated GABAergic synaptic plasticity, neural active ligand-receptor interaction, arachidonic acid metabolism and other fatty acid metabolic pathways to improve depression. A large number of experimental studies have shown that the nervous system function of GABA in patients with major depression was seriously damaged, and improving the nervous system function of GABA has is of significant antidepressant effect (Della Vecchia et al., 2022; Prevot and Sibille, 2021). Palmitic acid, adrenic acid, linoleic acid, arachidonic acid, 11,12-epoxyeicosenoic acid, docosapentaenoic acid belongs to the essential fatty acids of human body. Many researchers have reported that depression could be effectively treated by supplementing the essential fatty acids of human body and improving the metabolic process of fatty acids (Deacon et al., 2017; Hsu et al., 2018; Liao et al., 2019). Fatty acid amide hydrolase (FAAH) is an important enzyme to hydrolyze endocannabinoids and related amide-signaling lipids. Pharmacological studies have shown that FAAH is closely associated with mediating inflammatory response, pain, anxiety, depression and neurodegenerative diseases (Shang et al., 2022). FAAH inhibitors were anticipated to be a new type of antidepressant drugs (Tripathi, 2020). Epoxyeicosatrienoic acid signaling is an arachidonic acid metabolic pathway, and changes in specific brain regions have been observed in mouse models of depression and postmortem samples from patients with depression. With exposure to chronic social stress stimulation, prefrontal lobe enzyme activity of susceptible mice increased accompanied with weakened social interaction and depression-like behavior. EPHX2 could encode soluble epoxide hydrolase (sEH) and decreasing expression of EPHX2 could alleviate depressive symptoms (Xiong et al., 2019). In addition, sEH inhibitors produce

rapid antidepressant-like effects in a variety of animal models of depression, including chronic social failure stress and chronic mild stress (Swardfager et al., 2018; Wu et al., 2017).

Since the publication of the theory that gut microbes could regulate the brain-gut axis pathway to treat depression, researchers have focused on this field. This hypothesis initiates a new approach to study the physiological and pathological mechanism of depression. Since then, the interaction between the gut microbiome and the brain has gradually become the focus of neuroscience research (Liang et al., 2018). More and more studies have shown that gut microbiota could participate in the metabolic process of components from Chinese medicinals, while components from herbs could affect the metabolic function of gut microbiota (Zhang et al., 2021b). Chinese medicinals are mainly administered orally. Part of the active components of herbs would be directly absorbed into the blood, while other components enter the intestine and interacts with gut microbiota. On the one hand, gut microbiota could transform Chinese medicinals and change their biological activities, producing active substances with smaller molecular weight, higher bioavailability and better lipophilicity. On the other hand, components of Chinese medicinals could affect the structure, function and metabolism of gut microbiota, and had functions such as anti-inflammation, metabolic promotion and nerve regulation (Sousa et al., 2008). Gut microbiota and nervous system function are closely connected through various ways. The imbalance of gut microbiota structure could increase intestinal permeability and increase the level of inflammatory factors, which makes inflammatory factors more easily cross the brain-blood barrier and aggravate neuroinflammation and nerve injury. Probiotics could reduce intestinal permeability and reduce the content of inflammatory factors into the blood, so as to relieve the inflammatory damage of the nervous system (Leblhuber et al., 2021). The activation of HPA axis in the brain could increase the release of CORT, increase intestinal permeability, regulate endocrine cells, immune cells, cytokines and other factors affecting the gastrointestinal microenvironment, thus changing the structure and function of gut microbiota (Wang and Kasper, 2014). Small molecules in blood such as 5-HT, GABA, Glu, dopamine (DA), brain-derived neurotrophic factor (BDNF) and other components are produced by or regulated by gut microbiota. In addition, metabolites produced by gut microbiota could effectively degrade ammonia, phenols, amines, phenolic acids and other neurotoxic substances, or reduce the content of toxic substances, so as to prevent toxic substances from crossing the brain-blood barrier and damaging brain tissue (Averina et al., 2020; Parker et al., 2020; Zhu et al., 2020).

Based on the above theories, we innovatively put forward the conclusion that part of LBRD substance is directly absorbed into the blood, interacts with serum constituents and is metabolized into a variety of fatty acid components and amino acid components, while the other part, macromolecular substances could increase the abundance of *Bacteroides* and *Lactobacillus*, and promote the metabolism and transformation process of herbs components in the body, produce some active substances, reduce intestinal permeability, reduce inflammation level, regulate fatty acid, amino acid and other endogenous metabolic pathways, promote the synthesis and transport of neurotransmitter GABA, improve the nervous system function and play a neuroprotective role.

Most of the depression cell models are established by using chemical drugs or glucocorticoids to induce nerve cell damage. CORT-induced cell damage is widely used in establishing cell models of depression (Lee et al., 2020; Shen et al., 2021). CORT, a glucocorticoid, has the effect of maintaining the balance and stability of the body's physiological functions, and the elevated content of CORT would lead to excessive activation of the HPA axis, resulting in a series of reactions such as oxidative stress, glutamatergic excitatory toxicity and neuroinflammation, impairing nerve function and inhibiting neurogenesis, which is an important pathogenesis of depression (Bai et al., 2022; Lin et al., 2021; Liu et al., 2019; Spencer and Deak, 2017; Yang et al., 2022a). The deletion of 5-HT and the increase of cytokine levels in the peripheral nervous system would affect the metabolic process of Glu and lead to the

increase of Glu level, thus resulting in the imbalance of E/I and the decreased GABA level, which are involved in inducing depression. Remodeling E/I imbalance can improve the function of the nervous system and play a significant antidepressant role (Camargo et al., 2018; Freitas et al., 2016; Juruena et al., 2018; Keller et al., 2017). Therefore, we chose CORT damaged primary cortical neurons and two neuronal cell lines, PC12 and Neuro-2a cells, to establish cell models suitable for studying the pathogenesis of E/I imbalance and inflammatory injury in depression.

The *in vitro* cell experiment based on the theory of serum pharmacology is a common approach to study the pharmacodynamic mechanism of Chinese medicinal, and screening the optimal intervention concentration of Chinese medicinal drug-containing serum is a key step in the whole experiment. Too high or too low concentration of drug-containing serum may lead to negative or positive results falsely. The optimal concentration of drug-containing serum can also reduce the number of follow-up experiment groups and reduce operation errors. Therefore, screening the optimal concentration of drug-containing serum for intervention is of great significance for the *in vitro* cell experiments to study the pharmacological mechanism of botanical products. Therefore, we screened suitable concentrations of LBRDDS to intervene and protect cell models, and verified the protective effect of LBRDDS on CORT-induced cell models according to cell survival rate, LDH cytotoxicity, neurotransmitter and inflammatory factors. The experimental results showed that with CORT treatment, cell survival rate decreased significantly, the contents of 5-HT, GABA and IL-10 decreased, and the levels of Glu and IL-1 β increased. LBRDDS could increase the cell survival rate, reduce cytotoxicity, increase the contents of GABA, 5-HT and IL-10, decrease the levels of Glu and IL-1 β , restore the balance of E/I, reduce inflammation level, and protect nerve cells from CORT damage. GABA is the most important inhibitory neurotransmitter in mammalian central nervous system. Recently, the epigenetic changes linked to GABAergic deficit have been described in prefrontal cortex of depressive patients and chronically stressed animals' depression (Kolosowska et al., 2023). According to the results of qRT-PCR and western blotting, LBRDDS could inhibit the expression of miRNA-144-3p, increase the synthesis and transport function of GABA, so as to play an antidepressant role, while disturbing the expression of miRNA-144-3p could reverse the pharmacological effect of LBRDDS.

In this research, we established an *in vitro* cell model of depression by

CORT injury of nerve cells, and selected the best pharmacological concentration of LBRDDS to intervene the model cells. The changes of cell viability, neurotransmitters and cytokines were detected and compared with the previous experiments. The results showed that the trend of multiple indicators was consistent with the previous PC12 *in vitro* experiment and CUMS-induced mouse depression model, which indicated that we successfully constructed an *in vitro* cell model of depression. By negatively regulating miRNA-144-3p expression, LBRDDS can increase GABA synthesis and transport and improve nervous system function with antidepressant effect (Fig. 9).

There are some limitations of this research. First, LBRD has a variety of active ingredients, and the metabolic distribution and synergistic pharmacodynamic process after absorption into the blood are not clear. Second, the biological characteristics of primary cortical neurons resembles those of the cells in the original brain, and primary cortical neurons could maintain the major structure and function of brain tissues. Therefore, primary cortical neurons are more suitable for the study of neuropsychiatric diseases. However, due to various drawbacks, such as the high cost of cell culture, the difficulty of isolating cells, the slow growth rate and the short survival time, the application of primary cortical neurons is limited. Further, the mechanism between key target genes, active ingredients, intestinal flora, and neurotransmitter synthesis has not been verified in experiments *in vivo*. Finally, changes of flora, serum metabolites and pharmacodynamics after LBRD acting on animal models of depression are consistent with the results of this manuscript.

In future study, we will explore how depression could be treated by LBRD through regulating gut flora based on brain-gut microbial pathway. Firstly, molecular experiments were used to verify the regulatory relationship between key target genes, LBRD into blood active components and gut microbiota metabolism; secondly, animal experiments were used to verify the biological process of key probiotics *Bacteroides* and *Lactobacillus* promoting the secretion and synthesis of neurotransmitter GABA. It is proved that LBRD could regulate intestinal metabolic function, increase neurotransmitter secretion, reduce inflammation level, and play an antidepressant role by increasing the gut microbiota abundance of *Bacteroides* and *Lactobacillus*. In order to avoid the difficulty of primary neuron culture, organoid culture can be selected to induce stem cell differentiation for large-scale pharmacological mechanism screening. We will compare changes of serum and

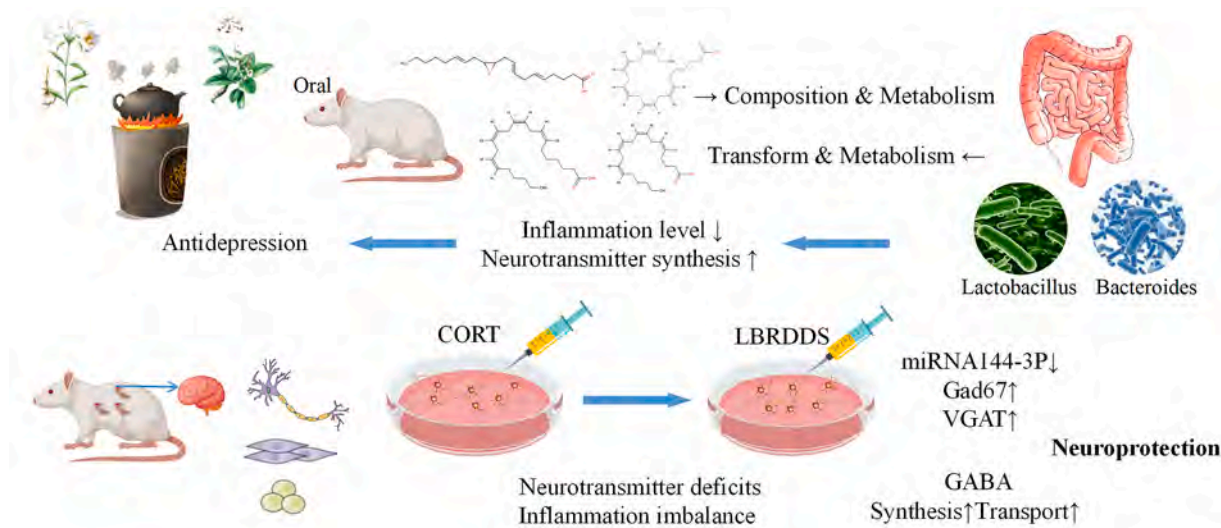


Fig. 9. Synergistic neuroprotective effects of *L. henryi* Baker and *R. glutinosa* (Gaertn.) DC. against CORT-induced nerve cell injury by correcting neurotransmitter deficits and inflammation imbalance. CORT injured nerve cells can be served as the cell model in which to research the depression mechanisms underlying neurotransmitter deficits and inflammation imbalance *in vitro* experiments. The potential effective compounds (LBRDDS) were absorbed from intestinal tract in human body through interactions between LBRD and gut microbiota. LBRDDS exerts neuroprotective effects by correcting neurotransmitter deficits and inflammation imbalance in the CORT-induced nerve cell injury model via regulating the miRNA-144-3p mediated GABA synthesis and release.

cerebrospinal fluid material components in depression model rats before and after LBRD treatment, and then find the material components in LBRD that can enter the blood and cross the cerebral blood barrier at the same time. It may also be possible to try to enter the brain through a new nano-mediated drug delivery system across the blood-brain barrier or to target miRNA into nerve cells through an improved viral vector as a new means of treating depression.

At present, “Chinmedomics” is a research strategy initiated by Professor Wang Xijun of Heilongjiang University of Traditional Chinese Medicine. It integrates the serum pharmacology of TCM and metabolomics technology to evaluate the effectiveness of TCM and discover the pharmacodynamic material basis related to effect, and therefore it has become one of the hot research directions in the field of international TCM and natural medicine research, and is an innovation in the sense of modern research methodology of TCM. The journal of *Nature* has also reported “Chinmedomics”, and holds that it has created a “language” for the communication between modern biology and TCM. Using this language TCM is no longer self-consistent in a closed theoretical system and realizes “dialogue” with modern science. In the future study, we will combine metabolomics research techniques and serum pharmacology to deeply explore the pharmacodynamic mechanism of the active ingredients of LBRD entering the blood, and provide more data support the innovative development and drug development of LBRD.

Conclusion

Overall, the current study proved that LBRDDS exerts neuroprotective effects by correcting neurotransmitter deficits and inflammation imbalance in the CORT-induced nerve cell injury model via improving the activity of model cells and regulating the miRNA-144-3p mediated GABA synthesis and release. These findings could provide the molecular basis for a developmental breakthrough in the natural medicinal plants (*L. henryi* Baker and *R. glutinosa*) as well as the pathogenesis of depression.

Data availability

The data presented in this study are available on request from the corresponding author.

Authorship contributions

All data were generated in-house, and no paper mill was used. All authors agree to be accountable for all aspects of work ensuring integrity and accuracy.

Ethics statement

The current study was performed with the approval of the Animal Ethics Committee of Shandong University of Traditional Chinese Medicine (SDUTCM20230629001) and performed in strict accordance with the Guide for the Care and Use of Laboratory animals published by the US National Institutes of Health. The approval date was July 1, 2023, and the effective date is June 31, 2024.

Funding

This study was granted by National Nature Science Foundation of China (82204795 and 81903948), the special fund for high-level talent cultivation project of traditional Chinese medicine in Shandong Province (2023-143), Shanghai Science and Technology Development Foundation (2023-701627), Shandong Province Universities' Development Plan for Youth Innovation Teams (2019-9-202 and 2022KJ340), Shandong Provincial Natural Science Foundation (ZR2020QH329).

Supplementary materials

Figure S1: Two plants were authenticated by Shandong Provincial Analysis and Testing Center using molecular biology techniques to compliment conventional methods.

Figure S2: Preparation of Lily Bulb and Rehmannia Decoction.

Figure S3: Gut microbiota alpha diversity index and predictive metabolic pathway regulated by LBRD.

Figure S4: Different concentrations of Blank serum and LBRDDS effects on Neuro-2a cells survival rate.

Figure S5: Effect of mifepristone (RU486) on cell viability and neurotransmitter levels in Neuro-2a cell injury model induced by CORT.

Figure S6: The pattern plot of the protein band in Figure 8 is derived from the whole un-cropped images of the original western blots.

Table S1: Gene primer sequence information.

Table S2: Characterization of the main chemical constituents in blank serum by UPLCQTOF-MS/MS.

Table S3: Characterization of the main chemical constituents in LBRD by UPLCQTOF-MS/MS.

Table S4: LBRD prototype into blood component.

Table S5: LBRD regulation by differential gut microbiota predicted metabolic pathways.

Table S6: Gut Microbiota suitable for LBRD active composition metabolism.

CRediT authorship contribution statement

Jin Pan: Conceptualization, Writing – original draft, Visualization, Investigation, Writing – review & editing. **Yanting Lu:** Writing – review & editing, Supervision, Funding acquisition. **Sijia Wang:** Visualization, Investigation. **Ting Ma:** Visualization, Investigation, Writing – review & editing. **Xiaoyan Xue:** Data curation, Validation. **Zhe Zhang:** Writing – review & editing, Supervision. **Qiancheng Mao:** Visualization, Investigation. **Dongjing Guo:** Data curation, Validation. **Ke Ma:** Writing – review & editing, Supervision, Funding acquisition.

Declaration of Competing Interest

The authors declare that they have no conflict of interest

Acknowledgment

All authors are grateful to Xiuyang Li, an expert in translating TCM terminology, helped us to correct and revise the contents related to TCM. We thank Wuhan Servicebio technology CO., LTD, for their excellent technical support. In addition, we also thank the English editors of Editage (www. editage. com).

Supplementary materials

Supplementary material associated with this article can be found, in the online version, at [doi:10.1016/j.phymed.2023.155102](https://doi.org/10.1016/j.phymed.2023.155102).

References

- Ahmed, S., Singh, S., Singh, V., Roberts, K.D., Zaidi, A., Rodriguez-Palacios, A., 2022. The Weissella genus: clinically treatable bacteria with antimicrobial/probiotic effects on inflammation and cancer. *Microorganisms* 10. <https://doi.org/10.3390/microorganisms10122427>.
- Averina, O.V., Zorkina, Y.A., Yunes, R.A., Kovtun, A.S., Ushakova, V.M., Morozova, A.Y., Kostyuk, G.P., Danilenko, V.N., Chekhonin, V.P., 2020. Bacterial metabolites of human gut microbiota correlating with depression. *Int. J. Mol. Sci.* 21. <https://doi.org/10.3390/ijms211239234>.
- Bai, G., Jing, S., Cao, H., Qiao, Y., Chen, G., Duan, L., Yang, Y., Li, M., Li, W., Chang, X., Yang, C., Wang, Q., 2022. Kai-Xin-San protects depression mice against Cort-induced neuronal injury by inhibiting microglia activation and oxidative stress. *Evid. Based Complement. Alternat. Med.* 2022, 5845800 <https://doi.org/10.1155/2022/5845800>.

- Bravo, J.A., Forsythe, P., Chew, M.V., Escaravage, E., Savignac, H.M., Dinan, T.G., Bienenstock, J., Cryan, J.F., 2011. Ingestion of *Lactobacillus* strain regulates emotional behavior and central GABA receptor expression in a mouse via the vagus nerve. *Proc. Natl. Acad. Sci. USA* 108, 16050–16055. <https://doi.org/10.1073/pnas.1102999108>.
- Brown, S.J., Brown, A.M., Purves-Tyson, T.D., Huang, X.F., Shannon Weickert, C., Newell, K.A., 2022. Alterations in the kynurenine pathway and excitatory amino acid transporter-2 in depression with and without psychosis: evidence of a potential astrocyte pathology. *J. Psychiatr. Res.* 147, 203–211. <https://doi.org/10.1016/j.jpsychires.2021.12.039>.
- Camargo, A., Dalmagro, A.P., Rikel, L., da Silva, E.B., Simao da Silva, K.A.B., Zeni, A.L.B., 2018. Cholecalciferol counteracts depressive-like behavior and oxidative stress induced by repeated corticosterone treatment in mice. *Eur. J. Pharmacol.* 833, 451–461. <https://doi.org/10.1016/j.ejphar.2018.07.002>.
- Cani, P.D., Bibiloni, R., Knaut, C., Waget, A., Neyrinck, A.M., Delzenne, N.M., Burcelin, R., 2008. Changes in gut microbiota control metabolic endotoxemia-induced inflammation in high-fat diet-induced obesity and diabetes in mice. *Diabetes* 57, 1470–1481. <https://doi.org/10.2337/db07-1403>.
- Chen, M.L., Gao, J., He, X.R., Chen, Q., 2012. Involvement of the cerebral monoamine neurotransmitters system in antidepressant-like effects of a chinese herbal decoction, baihe dihuang tang, in mice model. *Evid. Based Complement. Alternat. Med.* 419257 <https://doi.org/10.1155/2012/419257>, 2012.
- Chen, R., Xu, Y., Wu, P., Zhou, H., Lasanajak, Y., Fang, Y., Tang, L., Ye, L., Li, X., Cai, Z., Zhao, J., 2019. Transplantation of fecal microbiota rich in short chain fatty acids and butyric acid treat cerebral ischemic stroke by regulating gut microbiota. *Pharmacol. Res.* 148, 104403 <https://doi.org/10.1016/j.phrs.2019.104403>.
- Chi, X., Wang, S., Baloch, Z., Zhang, H., Li, X., Zhang, Z., Zhang, H., Dong, Z., Lu, Y., Yu, H., Ma, K., 2019. Research progress on classical traditional Chinese medicine formula Lily Bulb and Rehmannia Decoction in the treatment of depression. *Biomed. Pharmacother.* 112, 108616 <https://doi.org/10.1016/j.biopha.2019.108616>.
- Correia, A.S., Fraga, S., Teixeira, J.P., Vale, N., 2022. Cell model of depression: reduction of cell stress with mirtazapine. *Int. J. Mol. Sci.* 23 <https://doi.org/10.3390/ijms23094942>.
- Deacon, G., Kettle, C., Hayes, D., Dennis, C., Tucci, J., 2017. Omega 3 polyunsaturated fatty acids and the treatment of depression. *Crit. Rev. Food Sci. Nutr.* 57, 212–223. <https://doi.org/10.1080/10408398.2013.876959>.
- Della Vecchia, A., Arone, A., Piccinni, A., Mucci, F., Marazziti, D., 2022. GABA system in depression: impact on pathophysiology and psychopharmacology. *Curr. Med. Chem.* 29, 5710–5730. <https://doi.org/10.2174/092986732866621115124149>.
- Freitas, A.E., Egea, J., Buendia, I., Gomez-Rangel, V., Parada, E., Navarro, E., Casas, A.I., Wojnicz, A., Ortiz, J.A., Cuadrado, A., Ruiz-Nuno, A., Rodrigues, A.L.S., Lopez, M.G., 2016. Agmatine, by improving neuroplasticity markers and inducing Nrf2, prevents corticosterone-induced depressive-like behavior in mice. *Mol. Neurobiol.* 53, 3030–3045. <https://doi.org/10.1007/s12035-015-9182-6>.
- Gonda, X., Dome, P., Neill, J.C., Tarazi, F.I., 2023. Novel antidepressant drugs: beyond monoamine targets. *CNS Spectr.* 28, 6–15. <https://doi.org/10.1017/S1092852921000791>.
- Goodwin, G.M., Aaronson, S.T., Alvarez, O., Arden, P.C., Baker, A., Bennett, J.C., Bird, C., Blom, R.E., Brennan, C., Bruschi, D., Burke, L., Campbell-Coker, K., Carhart-Harris, R., Cattell, J., Daniel, A., DeBattista, C., Dunlop, B.W., Eisen, K., Feifel, D., Forbes, M., Haumann, H.M., Hellerstein, D.J., Hoppe, A.I., Husain, M.I., Jelen, L.A., Kamphuis, J., Kawasaki, J., Kelly, J.R., Key, R.E., Kishon, R., Knatz Peck, S., Knight, G., Koolen, M.H.B., Lean, M., Licht, R.W., Maples-Keller, J.L., Mars, J., Marwood, L., McElhiney, M.C., Miller, T.L., Mirows, A., Mistry, S., Mletzko-Crowe, T., Modlin, L.N., Nielsen, R.E., Nielson, E.M., Offerhaus, S.R., O'Keane, V., Palenicek, T., Printz, D., Rademaker, M.C., van Reemst, A., Reinholdt, F., Repantis, D., Rucker, J., Rudow, S., Ruffell, S., Rush, A.J., Schoevers, R.A., Seynaeve, M., Shao, S., Soares, J. C., Somers, M., Stansfield, S.C., Sterling, D., Strockis, A., Tsai, J., Visser, L., Wahba, M., Williams, S., Young, A.H., Ywema, P., Zisook, S., Malievskaja, E., 2022. Single-Dose psilocybin for a treatment-resistant episode of major depression. *N. Engl. J. Med.* 387, 1637–1648. <https://doi.org/10.1056/NEJMoa2206443>.
- Gorica, E., Calderone, V., 2022. Arachidonic acid derivatives and neuroinflammation. *CNS Neurol. Disord. Drug Targets* 21, 118–129. <https://doi.org/10.2174/1871527320666210208130412>.
- Grosso, G., Galvano, F., Marventano, S., Malaguarnera, M., Bucolo, C., Drago, F., Caraci, F., 2014. Omega-3 fatty acids and depression: scientific evidence and biological mechanisms. *Oxid. Med. Cell Longev* 2014, 313570. <https://doi.org/10.1155/2014/313570>.
- Hsu, M.C., Tung, C.Y., Chen, H.E., 2018. Omega-3 polyunsaturated fatty acid supplementation in prevention and treatment of maternal depression: putative mechanism and recommendation. *J. Affect. Disord.* 238, 47–61. <https://doi.org/10.1016/j.jad.2018.05.018>.
- Jha, M.K., Mathew, S.J., 2023. Pharmacotherapies for treatment-resistant depression: how antipsychotics fit in the rapidly evolving therapeutic landscape. *Am. J. Psychiatry* 180, 190–199. <https://doi.org/10.1176/appi.ajp.20230025>.
- Juruena, M.F., Bocharova, M., Agustini, B., Young, A.H., 2018. Atypical depression and non-atypical depression: Is HPA axis function a biomarker? A systematic review. *J. Affect. Disord.* 233, 45–67. <https://doi.org/10.1016/j.jad.2017.09.052>.
- Keiser, M.J., Roth, B.L., Armbruster, B.N., Ernsberger, P., Irwin, J.J., Shoichet, B.K., 2007. Relating protein pharmacology by ligand chemistry. *Nat. Biotechnol.* 25, 197–206. <https://doi.org/10.1038/nbt1284>.
- Jr. Keller, J., Gomez, R., Williams, G., Lembke, A., Lazzaroni, L., Murphy, G.M., Schatzberg, A.F., 2017. HPA axis in major depression: cortisol, clinical symptomatology and genetic variation predict cognition. *Mol. Psychiatry* 22, 527–536. <https://doi.org/10.1038/mp.2016.120>.
- Kolosowska, K.A., Schratz, G., Winterer, J., 2023. microRNA-dependent regulation of gene expression in GABAergic interneurons. *Front. Cell Neurosci.* 17, 1188574 <https://doi.org/10.3389/fncel.2023.1188574>.
- Larrieu, T., Laye, S., 2018. Food for mood: relevance of nutritional omega-3 fatty acids for depression and anxiety. *Front. Physiol.* 9, 1047. <https://doi.org/10.3389/fphys.2018.101047>.
- Leblhuber, F., Ehrlich, D., Steiner, K., Geisler, S., Fuchs, D., Lanser, L., Kurz, K., 2021. The Immunopathogenesis of Alzheimer's disease is related to the composition of gut microbiota. *Nutrients* 13. <https://doi.org/10.3390/nu13020361>.
- Lee, Y.J., Kim, H.R., Lee, C.Y., Hyun, S.A., Ko, M.Y., Lee, B.S., Hwang, D.Y., Ka, M., 2020. 2-Phenylethylamine (PEA) ameliorates corticosterone-induced depression-like phenotype via the BDNF/TrkB/CREB signaling pathway. *Int. J. Mol. Sci.* 21 <https://doi.org/10.3390/ijms21239103>.
- Li, Z., Lai, J., Zhang, P., Ding, J., Jiang, J., Liu, C., Huang, H., Zhen, H., Xi, C., Sun, Y., Wu, L., Wang, L., Gao, X., Li, Y., Fu, Y., Jie, Z., Li, S., Zhang, D., Chen, Y., Zhu, Y., Lu, S., Lu, J., Wang, D., Zhou, H., Yuan, X., Li, X., Pang, L., Huang, M., Yang, H., Zhang, W., Brix, S., Kristiansen, K., Song, X., Nie, C., Hu, S., 2022. Multi-omics analyses of serum metabolome, gut microbiome and brain function reveal dysregulated microbiota-gut-brain axis in bipolar depression. *Mol. Psychiatry* 27, 4123–4135. <https://doi.org/10.1038/s41380-022-01569-9>.
- Liang, S., Wu, X., Hu, X., Wang, T., Jin, F., 2018. Recognizing depression from the microbiota(-)gut(-)brain axis. *Int. J. Mol. Sci.* 19 <https://doi.org/10.3390/ijms19061592>.
- Liao, Y., Xie, B., Zhang, H., He, Q., Guo, L., Subramanieapillai, M., Fan, B., Lu, C., McIntyre, R.S., 2019. Efficacy of omega-3 PUFAs in depression: a meta-analysis. *Transl. Psychiatry* 9, 190. <https://doi.org/10.1038/s41398-019-0515-5>.
- Lin, R., Liu, L., Silva, M., Fang, J., Zhou, Z., Wang, H., Xu, J., Li, T., Zheng, W., 2021. Hederagenin protects PC12 cells against corticosterone-induced injury by the activation of the PI3K/AKT pathway. *Front. Pharmacol.* 12, 712876 <https://doi.org/10.3389/fphar.2021.712876>.
- Lin, S., Huang, L., Luo, Z.C., Li, X., Jin, S.Y., Du, Z.J., Wu, D.Y., Xiong, W.C., Huang, L., Luo, Z.Y., Song, Y.L., Wang, Q., Liu, X.W., Ma, R.J., Wang, M.L., Ren, C.R., Yang, J. M., Gao, T.M., 2022. The ATP level in the medial prefrontal cortex regulates depressive-like behavior via the medial prefrontal cortex-lateral habenula pathway. *Biol. Psychiatry* 92, 179–192. <https://doi.org/10.1016/j.biopsych.2022.02.014>.
- Liu, L., Dong, Y., Shan, X., Li, L., Xia, B., Wang, H., 2019. Anti-Depressive effectiveness of Baicalin *in vitro* and *in vivo*. *Molecules* 24. <https://doi.org/10.3390/molecules24020326>.
- Liu, Y., Yang, X., Gan, J., Chen, S., Xiao, Z.X., Cao, Y., 2022. CB-Dock2: improved protein-ligand blind docking by integrating cavity detection, docking and homologous template fitting. *Nucleic. Acids. Res.* 50, W159–W164. <https://doi.org/10.1093/nar/gkac394>.
- Liu, L., Wang, H., Chen, X., Zhang, Y., Zhang, H., Xie, P., 2023. Gut microbiota and its metabolites in depression: from pathogenesis to treatment. *EBioMedicine* 90, 104527. <https://doi.org/10.1016/j.ebiom.2023.104527>.
- Lu, K., Hong, Y., Tao, M., Shen, L., Zheng, Z., Fang, K., Yuan, F., Xu, M., Wang, C., Zhu, D., Guo, X., Liu, Y., 2023. Depressive patient-derived GABA interneurons reveal abnormal neural activity associated with HTR2C. *EMBO Mol. Med.* 15, e16364. <https://doi.org/10.15252/emmm.202216364>.
- Ma, K., Wang, X., Feng, S., Xia, X., Zhang, H., Rahaman, A., Dong, Z., Lu, Y., Li, X., Zhou, X., Zhao, H., Wang, Y., Wang, S., Baloch, Z., 2020. From the perspective of traditional Chinese medicine: treatment of mental disorders in COVID-19 survivors. *Biomed. Pharmacother.* 132, 110810 <https://doi.org/10.1016/j.biopha.2020.110810>.
- Medina-Rodriguez, E.M., Cruz, A.A., De Abreu, J.C., Beurel, E., 2023. Stress, inflammation, microbiome and depression. *Pharmacol. Biochem. Behav.* 227–228, 173561 <https://doi.org/10.1016/j.pbb.2023.173561>.
- Miao, M., Peng, M., Chen, H., Liu, B., 2019. Effects of Baihe Dihuang powder on chronic stress depression rat models. *Saudi J. Biol. Sci.* 26, 582–588. <https://doi.org/10.1016/j.sjbs.2018.12.002>.
- Mokhtari, T., 2022. Targeting autophagy and neuroinflammation pathways with plant-derived natural compounds as potential antidepressant agents. *Phytother. Res.* 36, 3470–3489. <https://doi.org/10.1002/ptr.7551>.
- Park, M.Y., Kim, S.J., Ko, E.K., Ahn, S.H., Seo, H., Sung, M.K., 2016. Gut microbiota-associated bile acid deconjugation accelerates hepatic steatosis in ob/ob mice. *J. Appl. Microbiol.* 121, 800–810. <https://doi.org/10.1111/jam.13158>.
- Parker, A., Fonseca, S., Carding, S.R., 2020. Gut microbes and metabolites as modulators of blood-brain barrier integrity and brain health. *Gut Microbes* 11, 135–157. <https://doi.org/10.1080/19490976.2019.1638722>.
- Prevot, T., Sibille, E., 2021. Altered GABA-mediated information processing and cognitive dysfunctions in depression and other brain disorders. *Mol. Psychiatry* 26, 151–167. <https://doi.org/10.1038/s41380-020-0727-3>.
- Regulska, M., Szuster-Gluszczyk, M., Trojan, E., Leskiewicz, M., Basta-Kaim, A., 2021. The emerging role of the double-edged impact of arachidonic acid derived eicosanoids in the neuroinflammatory background of depression. *Curr. Neuropharmacol.* 19, 278–293. <https://doi.org/10.2174/1570159X18666200807144530>.
- Rudzik, L., Ostrowska, L., Pawlak, D., Malus, A., Pawlak, K., Waszkiewicz, N., Szulc, A., 2019. Probiotic *Lactobacillus Plantarum* 299v decreases kynurenine concentration and improves cognitive functions in patients with major depression: a double-blind, randomized, placebo controlled study. *Psychoneuroendocrinology* 100, 213–222. <https://doi.org/10.1016/j.psyneuen.2018.10.010>.
- Shan, J., Hashimoto, K., 2022. Soluble epoxide hydrolase as a therapeutic target for neuropsychiatric disorders. *Int. J. Mol. Sci.* 23 <https://doi.org/10.3390/ijms23094951>.

- Shang, Y., Wang, M., Hao, Q., Meng, T., Li, L., Shi, J., Yang, G., Zhang, Z., Yang, K., Wang, J., 2022. Development of indole-2-carbonyl piperazine urea derivatives as selective FAAH inhibitors for efficient treatment of depression and pain. *Bioorg. Chem.* 128, 106031 <https://doi.org/10.1016/j.bioorg.2022.106031>.
- Shen, F., Song, Z., Xie, P., Li, L., Wang, B., Peng, D., Zhu, G., 2021. Polygonatum sibiricum polysaccharide prevents depression-like behaviors by reducing oxidative stress, inflammation, and cellular and synaptic damage. *J. Ethnopharmacol.* 275, 114164 <https://doi.org/10.1016/j.jep.2021.114164>.
- Shi, X., Zhou, N., Cheng, J., Shi, X., Huang, H., Zhou, M., Zhu, H., 2019. Chlorogenic acid protects PC12 cells against corticosterone-induced neurotoxicity related to inhibition of autophagy and apoptosis. *BMC Pharmacol. Toxicol.* 20, 56. <https://doi.org/10.1186/s40360-019-0336-4>.
- Slykerman, R.F., Hood, F., Wickens, K., Thompson, J.M.D., Barthow, C., Murphy, R., Kang, J., Rowden, J., Stone, P., Crane, J., Stanley, T., Abels, P., Purdie, G., Maude, R., Mitchell, E.A., 2017. Effect of lactobacillus rhamnosus HN001 in pregnancy on postpartum symptoms of depression and anxiety: a randomised double-blind placebo-controlled trial. *EBioMedicine* 24, 159–165. <https://doi.org/10.1016/j.ebiom.2017.09.013>.
- Sousa, T., Paterson, R., Moore, V., Carlsson, A., Abrahamsson, B., Basit, A.W., 2008. The gastrointestinal microbiota as a site for the biotransformation of drugs. *Int. J. Pharm.* 363, 1–25. <https://doi.org/10.1016/j.ijpharm.2008.07.009>.
- Spencer, R.L., Deak, T., 2017. A users guide to HPA axis research. *Physiol. Behav.* 178, 43–65. <https://doi.org/10.1016/j.physbeh.2016.11.014>.
- Strandwitz, P., Kim, K.H., Terekhova, D., Liu, J.K., Sharma, A., Levering, J., McDonald, D., Dietrich, D., Ramadhar, T.R., Lekbua, A., Mroue, N., Liston, C., Stewart, E.J., Dubin, M.J., Zengler, K., Knight, R., Gilbert, J.A., Clardy, J., Lewis, K., 2019. GABA-modulating bacteria of the human gut microbiota. *Nat. Microbiol.* 4, 396–403. <https://doi.org/10.1038/s41564-018-0307-3>.
- Swardfager, W., Hennebel, M., Yu, D., Hammock, B.D., Levitt, A.J., Hashimoto, K., Taha, A.Y., 2018. Metabolic/inflammatory/vascular comorbidity in psychiatric disorders; soluble epoxide hydrolase (sEH) as a possible new target. *Neurosci. Biobehav. Rev.* 87, 56–66. <https://doi.org/10.1016/j.neubiorev.2018.01.010>.
- Tette, F.M., Kwofie, S.K., Wilson, M.D., 2022. Therapeutic anti-depressant potential of microbial GABA produced by lactobacillus rhamnosus strains for GABAergic signaling restoration and inhibition of addiction-induced HPA axis hyperactivity. *Curr. Issues Mol. Biol.* 44, 1434–1451. <https://doi.org/10.3390/cimb44040096>.
- Tripathi, R.K.P., 2020. A perspective review on fatty acid amide hydrolase (FAAH) inhibitors as potential therapeutic agents. *Eur. J. Med. Chem.* 188, 111953 <https://doi.org/10.1016/j.ejmech.2019.111953>.
- Wang, Y., Kasper, L.H., 2014. The role of microbiome in central nervous system disorders. *Brain Behav. Immun.* 38, 1–12. <https://doi.org/10.1016/j.bbi.2013.12.015>.
- Wang, Y.S., Shen, C.Y., Jiang, J.G., 2019. Antidepressant active ingredients from herbs and nutraceuticals used in TCM: pharmacological mechanisms and prospects for drug discovery. *Pharmacol. Res.* 150, 104520 <https://doi.org/10.1016/j.phrs.2019.104520>.
- Wu, Q., Cai, H., Song, J., Chang, Q., 2017. The effects of sEH inhibitor on depression-like behavior and neurogenesis in male mice. *J. Neurosci. Res.* 95, 2483–2492. <https://doi.org/10.1002/jnr.24080>.
- Xia, B., Chen, C., Tao, W., 2021. Neuroplasticity: a key player in the antidepressant action of Chinese herbal medicine. *Am. J. Chin. Med.* 49, 1115–1133. <https://doi.org/10.1142/S0192415X21500531>.
- Xiao, W., Su, J., Gao, X., Yang, H., Weng, R., Ni, W., Gu, Y., 2022. The microbiota-gut-brain axis participates in chronic cerebral hypoperfusion by disrupting the metabolism of short-chain fatty acids. *Microbiome* 10, 62. <https://doi.org/10.1186/s40168-022-01255-6>.
- Xiong, W., Cao, X., Zeng, Y., Qin, X., Zhu, M., Ren, J., Wu, Z., Huang, Q., Zhang, Y., Wang, M., Chen, L., Turecki, G., Mechawar, N., Chen, W., Yi, G., Zhu, X., 2019. Astrocytic epoxyeicosatrienoic acid signaling in the medial prefrontal cortex modulates depressive-like behaviors. *J. Neurosci.* 39, 4606–4623. <https://doi.org/10.1523/JNEUROSCI.3069-18.2019>.
- Xue, X., Pan, J., Zhang, H., Lu, Y., Mao, Q., Ma, K., 2022. Baihe Dihuang (*Litium henryi* Baker and *Rehmannia glutinosa*) decoction attenuates somatostatin interneurons deficits in prefrontal cortex of depression via miRNA-144-3p mediated GABA synthesis and release. *J. Ethnopharmacol.* 292, 115218 <https://doi.org/10.1016/j.jep.2022.115218>.
- Yang, L., Wang, Y., An, L., Zhang, X., Wang, J., Wang, Y., Cheng, R., Li, C., Ma, W., 2022a. Protective effect of schisandrin on CORT-induced PC12 depression cell model by inhibiting cell apoptosis *in vitro*. *Appl. Bionics Biomech.* 2022, 6113352 <https://doi.org/10.1155/2022/6113352>.
- Yang, X., Liu, Y., Gan, J., Xiao, Z.X., Cao, Y., 2022b. FitDock: protein-ligand docking by template fitting. *Brief Bioinform.* 23. <https://doi.org/10.1093/bib/bbac087>.
- Zhang, H., Chi, X., Pan, W., Wang, S., Zhang, Z., Zhao, H., Wang, Y., Wu, Z., Zhou, M., Ma, S., Zhao, Q., Ma, K., 2020. Antidepressant mechanism of classical herbal formula lily bulb and Rehmannia decoction: insights from gene expression profile of medial prefrontal cortex of mice with stress-induced depression-like behavior. *Genes Brain Behav.* 19, e12649. <https://doi.org/10.1111/gbb.12649>.
- Zhang, H., Xue, X., Pan, J., Song, X., Chang, X., Mao, Q., Lu, Y., Zhao, H., Wang, Y., Chi, X., Wang, S., Ma, K., 2021a. Integrated analysis of the chemical-material basis and molecular mechanisms for the classic herbal formula of lily bulb and rehmannia decoction in alleviating depression. *Chin. Med.* 16, 107. <https://doi.org/10.1186/s13020-021-00519-x>.
- Zhang, H.Y., Tian, J.X., Lian, F.M., Li, M., Liu, W.K., Zhen, Z., Liao, J.Q., Tong, X.L., 2021b. Therapeutic mechanisms of traditional Chinese medicine to improve metabolic diseases via the gut microbiota. *Biomed. Pharmacother.* 133, 110857 <https://doi.org/10.1016/j.biopha.2020.110857>.
- Zhang, J.C., Yao, W., Hashimoto, K., 2022a. Arketamine, a new rapid-acting antidepressant: a historical review and future directions. *Neuropharmacology* 218, 109219. <https://doi.org/10.1016/j.neuropharm.2022.109219>.
- Zhang, Y., Fan, Q., Hou, Y., Zhang, X., Yin, Z., Cai, X., Wei, W., Wang, J., He, D., Wang, G., Yuan, Y., Hao, H., Zheng, X., 2022b. Bacteroides species differentially modulate depression-like behavior via gut-brain metabolic signaling. *Brain Behav. Immun.* 102, 11–22. <https://doi.org/10.1016/j.bbi.2022.02.007>.
- Zhao, H.Q., Liu, J., Meng, P., Yang, H., Lin, X.Y., Long, H.P., Yu, X.M., Wang, Y.H., 2021. Effect of Baihe Dihuang Decoction on synaptic plasticity of hippocampus in rats with anxious depression. *Zhongguo Zhong Yao Za Zhi* 46, 1205–1210. <https://doi.org/10.19540/j.cnki.cjcm.20201221.401>.
- Zheng, W., Wang, G., Zhang, Z., Wang, Z., Ma, K., 2020. Research progress on classical traditional Chinese medicine formula Liuwei Dihuang pills in the treatment of type 2 diabetes. *Biomed. Pharmacother.* 121, 109564 <https://doi.org/10.1016/j.biopha.2019.109564>.
- Zhu, S., Jiang, Y., Xu, K., Cui, M., Ye, W., Zhao, G., Jin, L., Chen, X., 2020. The progress of gut microbiome research related to brain disorders. *J. Neuroinflammation* 17, 25. <https://doi.org/10.1186/s12974-020-1705-z>.
- Zununi Vahed, S., Barzegari, A., Rahbar Saadat, Y., Goreyshi, A., Omid, Y., 2017. Leuconostoc mesenteroides-derived anticancer pharmaceuticals hinder inflammation and cell survival in colon cancer cells by modulating NF-kappaB/AKT/PTEN/MAPK pathways. *Biomed. Pharmacother.* 94, 1094–1100. <https://doi.org/10.1016/j.biopha.2017.08.033>.